



# Soil phosphorus forms and storage in stormwater treatment areas of the Everglades: Influence of vegetation and nutrient loading

K.R. Reddy<sup>a,\*</sup>, Lilit Vardanyan<sup>a</sup>, Jing Hu<sup>a</sup>, Odi Villapando<sup>b</sup>, Rupesh K. Bhomia<sup>a</sup>, Taylor Smith<sup>a</sup>, W.G. Harris<sup>a</sup>, Sue Newman<sup>b</sup>

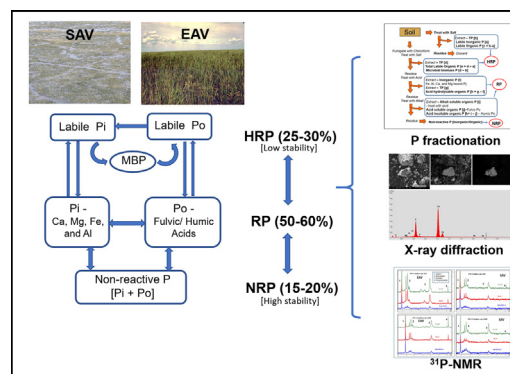
<sup>a</sup> University of Florida-IFAS, United States of America

<sup>b</sup> South Florida Water Management District, United States of America

## HIGHLIGHTS

- P fractionation, <sup>31</sup>P-NMR and x-ray diffraction were applied in this study to determine P forms, storage, and stability.
- HRP, RP and NRP pools account for 25–30, 50–60, and 15–20% of TP, respectively.
- Within HRP and RP pools, a large portion of P in the SAV was inorganic while organic P was more dominant in the EAV areas.

## GRAPHICAL ABSTRACT



## ARTICLE INFO

### Article history:

Received 10 January 2020

Received in revised form 1 April 2020

Accepted 2 April 2020

Available online 4 April 2020

### Keywords:

P fractionation

Phosphorus NMR

X-ray diffraction

Emergent aquatic vegetation

Submerged aquatic vegetation

## ABSTRACT

Stormwater treatment areas (STAs) are an integral component of the Everglades restoration strategies to reduce phosphorus (P) loads from adjacent agricultural and urban areas. The overall objective of this study was to determine the forms and distribution of P in floc and soils along the flow-path of two parallel flow-ways (FWs) in STA-2 with emergent aquatic vegetation (EAV) and submerged aquatic vegetation (SAV), respectively, to assess their stability and potential for long term storage. In EAV high organic matter accretion supported low bulk density and high P concentrations in floc and soil, while high mineral matter accretion in SAV resulted in high bulk density and low P concentrations. Approximately 25–30% of the total P is identified as highly reactive P (HRP) pools, 50–60% in moderately reactive P (RP) forms, and 15–20% in the non-reactive P (NRP) pool. Within HRP and RP pools, a large proportion of P in the SAV areas was inorganic while organic P was more dominant in the EAV areas. Enrichment of total P (especially in HRP and RP pools) found in the upstream areas of both FWs resulted from the P loading into FWs over time, and the surplus P conditions can potentially support flux into the water column. In EAV FW, approximately 45% of the P retained was recovered in floc and RAS and remaining was possibly retained in the above and below ground biomass and incorporated into subsurface soils. In SAV FW, all of the P retained was recovered in floc and soils suggesting P retention in plants was not significant. For STAs to continue to function effectively and meet the desired outflow TP concentrations, management strategies should be aimed to promote P limiting conditions within the system to avoid release of P from floc and soils to water column and potential downstream transport.

© 2020 Elsevier B.V. All rights reserved.

\* Corresponding author at: 2181 McCarty Hall, PO Box 110290, University of Florida, Gainesville, FL 32611, United States of America.  
E-mail address: [krr@ufl.edu](mailto:krr@ufl.edu) (K.R. Reddy).

## 1. Introduction

Phosphorus (P) storage and transformations in wetlands are influenced by organic and mineral matter inputs from external and internal sources (Kadlec and Wallace, 2009; Reddy and DeLaune, 2008; Reddy et al., 2005). Phosphorus retained in wetlands is present both in organic and inorganic forms and stored for short-term in vegetation and periphyton and for long-term in soils. A series of biotic and abiotic biogeochemical processes regulate reactivity and stability of these P forms stored in soils and the water column (Noe et al., 2002, 2001; Reddy et al., 1999; Reddy and DeLaune, 2008; Ruttenberg, 2003). Understanding the functional nature of different P pools is critical to developing strategies to improve the long-term sustainability of wetlands to retain P and associated elements (Condrón et al., 2005; Kadlec and Wallace, 2009; Reddy and DeLaune, 2008; Turner et al., 2006).

Inorganic P (Pi) and organic P (Po) forms in soils are usually determined by sequential extractions including acid and alkaline reagents (Bhomia and Reddy, 2018; Hedley and Stewart, 1982; Hieltjes and Lijklema, 1980; Ivanoff et al., 1998; Olila et al., 1995; Reddy et al., 2013; Ruttenberg, 1992; Yang and Post, 2011). These schemes typically identify P in the following groups: (1) highly reactive P pools as loosely-bound Pi, microbial biomass P, and labile Po; (2) moderately reactive P as; Pi associated with metals including Fe, Al, Ca, and Mg; and acid and alkali-extractable organic P (fulvic- and humic-bound P); and (3) non-reactive residual P. Because fractionation procedures are based on different solubilities of various P forms in different extractants, the chemically separated fractions are considered operationally defined. However, despite the limitations of P fractionation techniques, these approaches can provide semi-quantitative information to assess the potential stability and importance of different soil P fractions, particularly when combined with complementary approaches (Condrón and Newman, 2011). These complementary approaches include  $^{31}\text{P}$  nuclear magnetic resonance (NMR) spectroscopy, P K-edge X-ray absorption near edge structure (XANES) spectroscopy and two solid-state techniques – X-ray diffraction (XRD) and scanning electron microscopy (SEM) augmented with energy-dispersive X-ray fluorescence spectroscopy (EDS). These approaches provide confirmation of specific organic and inorganic P forms identified via P fractionation (Cade-Menun and Liu, 2014a; Cheesman et al., 2013; Harris and White, 2008; Koch et al., 2018).

Wetlands such as Stormwater Treatment Areas (STAs) accrete organic and mineral matter that contain organic and inorganic P forms and the interaction between these two pools results in release or retention of P in the system (Bhomia et al., 2015; Bhomia and Reddy, 2018; Reddy et al., 2005). The relative proportion and lability of organic and inorganic P pools are influenced by vegetation type, nutrient loading, and chemical composition of accreted material (Andersen et al., 2017; Bhomia and Reddy, 2018; Reddy et al., 1998; Yang and Post, 2011). Long-term P storage in wetlands relies upon the ability of soils to retain P in both organic and inorganic forms. Therefore, to determine the performance and sustainability of treatment wetlands, it is important to understand the stability and reactivity of various P pools in soils and its potential influence on surface water quality.

The primary question posed in this study is how and to what extent do the type of vegetation and nutrient loading influenced the forms, reactivity and storage of P in accreted soils. It is hypothesized that (1) emergent aquatic vegetation (EAV) and submerged aquatic vegetation (SAV) systems support different biogeochemical processes that affected the relative proportion of organic and inorganic P forms in the accreted material and (2) steady external nutrient loads result in higher labile pools of soil P in upstream areas of the STA.

We tested these hypotheses by determining the forms and distribution of P in floc and recently accreted soil (RAS) along two parallel FWs in STA-2, one of the five STAs established in strategic locations at the interface of the Everglades Agricultural Area and the Water Conservation Areas to reduce total P concentrations in surface water prior to

discharging that water into the Everglades Protection Area (Chimney, 2019).

## 2. Materials and methods

### 2.1. Site description

The study was conducted in STA-2 FWs 1 and 3. These are two good performing FWs (having achieved outflow TP concentration of  $20 \mu\text{g L}^{-1}$  or lower) with different vegetation communities and soil characteristics. The FW 1 was never farmed while most of the FW 3 was previously farmed except for 25% of the treatment area in the southeastern portion of the FW. STA-2 FW 1 is a single cell FW with a treatment area of 743 ha. It has predominantly emergent aquatic vegetation (EAV) consisting primarily of cattail (*Typha domingensis*) with patches of sawgrass (*Cladium jamaicense*) and water lily (*Nymphaea odorata*). The top 10 cm of the soil in the FW is highly organic. STA-2 FW 3 is also a single cell FW with a treatment area of 928 ha. It has predominantly submerged aquatic vegetation (SAV) with a large patch of EAV (primarily cattail with patches of sawgrass) in the southeastern region of the FW. The pre-STA soil in the FW 3 is highly organic but the current surface substrate is predominantly inorganic floc on top of inorganic RAS. Flow-ways 1 and 3 are operated as parallel treatment flow-ways and receive inflows originating from the same source/watershed.

Long term hydraulic loading rates to FW 1 and 3 are 2.6 and  $3.9 \text{ cm day}^{-1}$  and P loadings are 0.91 and  $1.33 \text{ g m}^{-2} \text{ yr}^{-1}$ . Each FW is managed at an average water depth of 0.38 and 0.55 m in FW 1 and FW 3. Range of values presented for each FW are in the same range as those reported for the whole STA-2 (Table 1).

### 2.2. Soil sampling

Intact soil cores from 11 transect stations in STA-2 FWs 1 and 3 were taken using a push-core method in September 2016 (Fig. 1). The inflow, midflow, and outflow locations along each transect, where triplicate soil cores were collected, were designated as benchmark sites. The soil cores were sectioned into floc (unconsolidated surficial sediments), RAS, and pre-STA soil (sectioned into 0–5 and 5–15 cm depths). Floc and RAS depths were determined as described by Reddy et al. (2019). Pre-STA soil represents the peat soil prior to STA construction. All samples were stored at  $4^\circ\text{C}$  until used for chemical analysis.

### 2.3. Physico-chemical analysis

Total carbon (TC) and total nitrogen (TN) were measured from dried, ground samples using Flash EA 1112 Elemental Analyzer (CE Instruments, Saddlebrook, NJ). Total P was analyzed by a combination of sample ignition at  $550^\circ\text{C}$  and acid digestion to convert organic P into inorganic P, followed by measurement of inorganic P in digestates

**Table 1**

Hydraulic and nutrient loading characteristics of FW 1 and FW 3 of STA-2 during operational period of WY2002–WY2017 (Zhao and Piccone, 2020). Data for whole STA-2 was obtained from the District SFER reports.  
(Source: South Florida Water Management District).

Parameter	FW 1 (EAV)	FW 3 (SAV)
Hydraulic loading rate ( $\text{cm d}^{-1}$ )	$2.6 \pm 1.2$	$3.9 \pm 1.2$
Water depth (m)	$0.38 \pm 0.12$	$0.55 \pm 0.08$
Hydraulic retention time (d)	$16 \pm 4$	$15 \pm 5$
Inflow TP ( $\mu\text{g L}^{-1}$ )	$92 \pm 25$	$94 \pm 34$
Outflow TP ( $\mu\text{g L}^{-1}$ )	$13 \pm 10$	$15 \pm 5$
Phosphorus loading rate ( $\text{g m}^{-2} \text{ yr}^{-1}$ )	$0.91 \pm 0.40$	$1.33 \pm 0.48$
Phosphorus retention rate ( $\text{g m}^{-2} \text{ yr}^{-1}$ )	$0.78 \pm 0.42$	$1.06 \pm 0.42$
STA-2 Hydraulic loading rate ( $\text{cm d}^{-1}$ )	$2.8 \pm 0.7$ (WY2004–WY2018)	
STA-2 Phosphorus loading rate ( $\text{g m}^{-2} \text{ yr}^{-1}$ )	$1.09 \pm 0.44$ (WY2004–WY2018)	
STA-2 Inflow - TP ( $\mu\text{g L}^{-1}$ )	$106 \pm 29$ (WY2004–WY2018)	
STA-2 Outflow - TP ( $\mu\text{g L}^{-1}$ )	$22 \pm 9$ (WY2004–WY2018)	

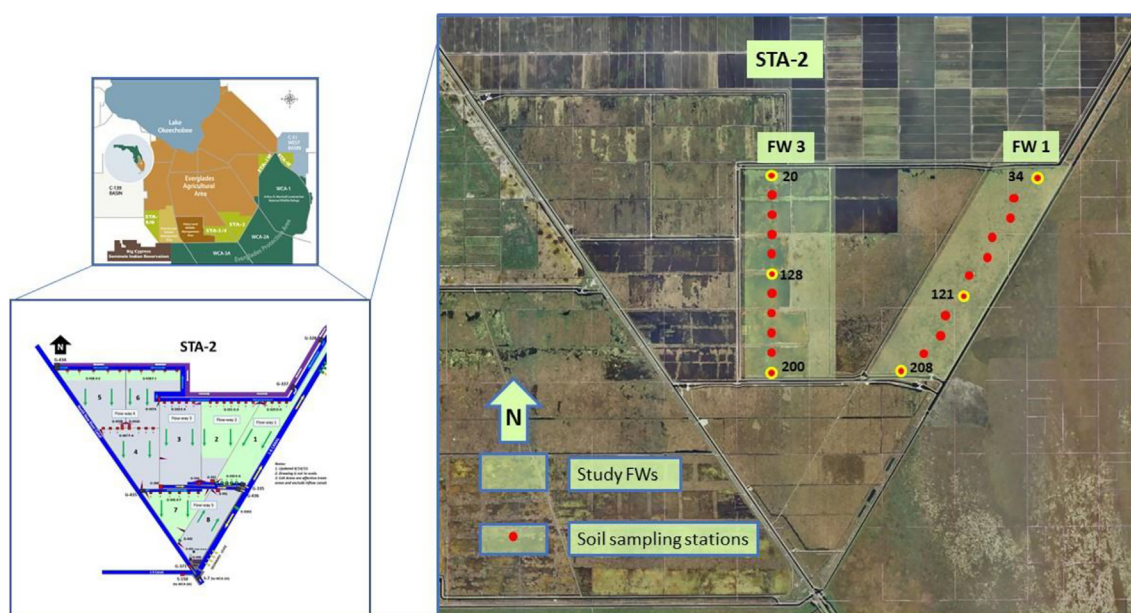


**Fig. 1.** Map showing the transect points in STA-2 FWs 1 and 3. FW1 consists of emergent aquatic vegetation (EAV) and FW 3 consists of submerged aquatic vegetation (SAV). Sampling locations along the flow-path are shown in red circles.

(USEPA, 1983; Method 365.1). Total inorganic P and acid-hydrolyzable organic P in soils was extracted with 1 M HCl (soil to solution ratio = 1:50; 3 h extraction time), filtered through a 0.45  $\mu\text{m}$  Millipore membrane filter and analyzed for SRP using a UV-visible spectrophotometer (Shimadzu, Norcross, Ga; USEPA, 1983; Method 365.1). These filtered extracts were analyzed for P, Ca, Mg, Fe, and Al using inductively coupled argon plasma spectrometry (ICAP). The ICAP analysis of P in HCl extracts represents the sum of inorganic P and acid-hydrolyzable organic P, while SRP measured spectrophotometrically with ammonium molybdate-ascorbic acid represents inorganic P (USEPA, 1983; Method 365.1). The difference between these two analyses is an estimate of acid-hydrolyzable organic P.

#### 2.4. Soil phosphorus fractionation

The soil P fractionation procedure used in the study is based on the solubility of inorganic and organic P pools in either acid or alkali solutions (Ivanoff et al., 1998; Reddy et al., 2013). This method has been used in several studies of wetland soils to operationally define P five discrete pools: (1) labile, (2) microbial, (3) acid-extractable, (4) alkali-extractable, and (5) residual (non-reactive to alkali and acids) (Fig. 2). These discrete pools of P were classified into three broad groups: Highly Reactive P (HRP) = bicarbonate extractable inorganic and organic P and microbial biomass P (MBP); Reactive P (RP) = acid extractable inorganic and organic P and alkali extractable organic P; Non-Reactive P (NRP) = P not extracted with either acid or alkali (Fig. 2).

#### 2.5. $^{31}\text{P}$ nuclear magnetic resonance spectroscopy

Floc and soil samples were dried at 35  $^{\circ}\text{C}$  about a week until mass constancy and extracted in a single step (Cade-Menun and Liu, 2014; Cheesman et al., 2013) with a solution containing 0.25 M NaOH and 0.05 M EDTA (in sodium salt form) using a soil to solution ratio of 1:20 and equilibrated on a mechanical shaker for 16 h at 20  $^{\circ}\text{C}$ . Soil suspensions were centrifuged at 11,200  $\times g$  for 15 min. A portion of supernatant solutions was digested and analyzed for total P (USEPA, 1983; Method 365.1) and the remaining extracts were frozen and stored at  $-4^{\circ}\text{C}$  for  $^{31}\text{P}$  NMR analysis (Cheesman et al., 2013).

#### 2.6. X-ray diffraction and Electron microscopy

RAS samples from six benchmark sites were evaluated for mineral constituents using X-ray powder diffraction (XRD) analysis (Harris and White, 2008). This analysis used a computer-controlled X-ray diffractometer (Ultima IV X-ray Diffractometer, Rigaku Corporation, Japan) equipped with stepping motor and graphite crystal monochromator. Samples were scanned from 2 to 60  $^{\circ} 2\theta$  at a rate of 2  $^{\circ} 2\theta$  per minute using Cu K $\alpha$  radiation. Minerals were identified by referencing XRD data for minerals published by the Joint Committee on Powder Diffraction Standards (<http://id.loc.gov/authorities/names/n78034813.html>).

Two samples (RAS of EAV inflow and midflow) were analyzed with a scanning electron microscope in conjunction with energy-dispersive X-ray fluorescence elemental spectroscopy (SEM-EDS) based on relatively high P concentration among the samples submitted. Samples were applied as a dry powder onto a carbon (C) adhesive tape mounted on a cylindrical stub. The mounted powders were coated with a thin C film to promote electron conduction and minimize charge buildup on surfaces. The SEM images and EDS analyses (elemental spectra and dot maps) were obtained from a FEI Nova NanoSEM 430 field emission scanning electron microscope equipped with an EDS detector (Harris et al., 2019).

#### 2.7. Statistical analysis

Statistical analyses were performed using JMP Pro 14 statistical software (SAS Institute Inc., Cary, NC). Mean and standard error from the three sampling locations at benchmark sites were calculated for four depths (floc, RAS, pre-STA1 0–5 cm, and pre-STA2 5–15 cm). A repeated measures linear model tested mean differences in P concentration of different pools for floc and soils from benchmark stations. Floc and soils at different depths of the same soil core were considered as repeated measures for the location of this core because these samples are likely to be correlated. Three factors were included in the model: depth, sampling stations (inflow, midflow, and outflow), and vegetation types (EAV and SAV). An unstructured repeated covariance structure was used to model the correlation among four sample types taken from the same soil core. Log transformation was applied, when needed, to satisfy normality assumptions of ANOVA. Tukey's test was conducted for multiple means comparisons. A Spearman's rank correlation analysis

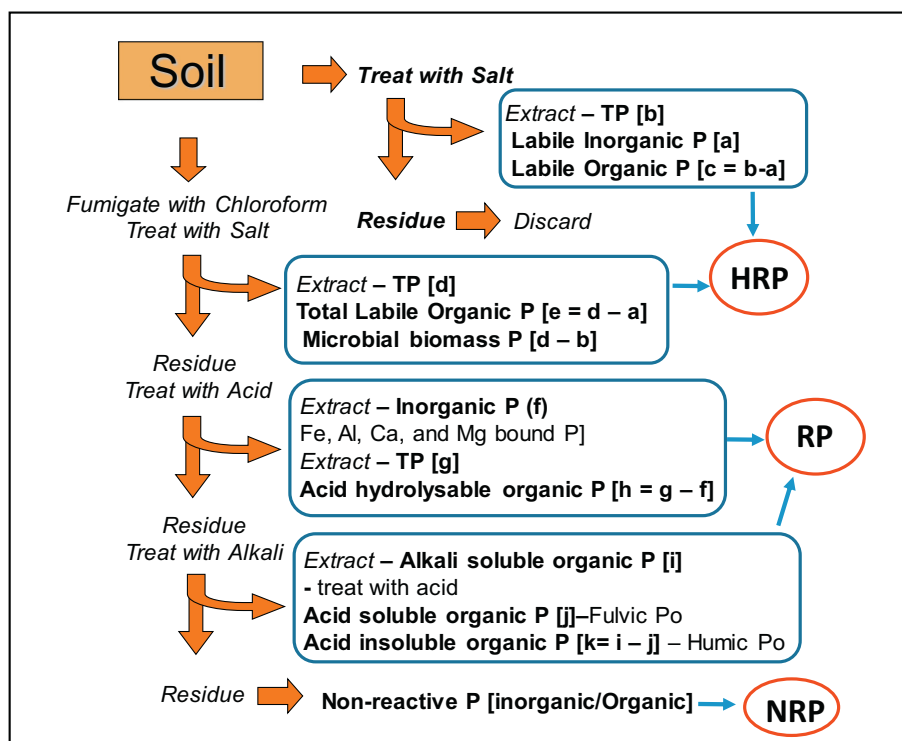


**Fig. 2.** Schematic showing operationally defined soil P fractionation scheme used in wetland soils (modified from Ivanoff et al., 1998 and Reddy et al., 2013). HRP = highly reactive; RP = moderately reactive P; and NRP = non-reactive P. Please refer to Table 2 for details of various P fractions.

was used to evaluate relationships among P forms and soil properties. A principal component analysis (PCA) was performed on the dataset to bring out strong patterns in different P fractions and other biogeochemical properties as a function of vegetation and fractional distance of sampling locations from inflow.

### 3. Results

#### 3.1. Physico-chemical properties

Floc depth decreased with distance from inflow in the EAV FW while no consistent trend was observed in the SAV FW (Table 2). RAS depth in both FWs was highest at the inflow station and was similarly low at the midflow and outflow locations (Table 2). Floc and RAS bulk densities were significantly higher in SAV than EAV (Table 2,  $P < 0.001$ ). Pre-STA soils at both depths generally showed higher bulk densities than RAS and floc layers in EAV and SAV systems (Tables 2 and 3). Soil organic carbon content (as indicated by loss on ignition) was significantly higher in EAV than SAV samples (Table 2,  $P < 0.001$ ). Total C (TC) concentrations in floc and RAS were two-fold higher in EAV than SAV system (Table 2) but were lower than TC concentrations in pre-STA soils of EAV and SAV (Tables 2 and 3). Total N concentrations in the floc and RAS of EAV were 2 to 3 times higher than SAV, while TN concentrations were similar in pre-STA soils of both systems (Tables 2 and 3).

#### 3.2. Phosphorus forms

Total P concentrations were significantly higher in floc and RAS of the EAV compared to the SAV system (Table 2,  $P < 0.001$ ) and decreased with depth and distance in both FWs (Fig. 3). Total P concentrations showed no distinct gradients along the flow-path in pre-STA soils (Fig. 3). Phosphorus concentrations in various pools were significantly affected by depth, station, and vegetation (Fig. 4).

##### 3.2.1. Highly reactive phosphorus [HRP]

Highly reactive inorganic P (HRPi) (also referred as labile Pi) in floc and RAS of EAV and SAV decreased with distance from inflow ( $P < 0.05$ , Fig. 4). Labile Pi in floc accounted for up to 15% of the total P in EAV and up to 25% in SAV at the inflow region of the FW and decreased with distance downstream (Fig. 5a). Labile Pi in EAV RAS accounted for <5% of the total P and was relatively steady along the

**Table 2**

Select physico-chemical properties of floc and RAS from benchmark locations in EAV (FW 1) and SAV (FW 3) flow-ways. Data are presented in the form of mean  $\pm$  standard error ( $n = 11$ ). Vegetation and depth are two factors included in the two-way ANOVA. Values not connected by same letter for each parameter (4 values in the same row) are significantly different (Tukey's test,  $\alpha = 0.05$ ). The level of significant differences between EAV and SAV is denoted by the asterisks following each parameter (NS: not significantly different; \* $P < 0.05$ ; \*\* $P < 0.01$ ; \*\*\* $P < 0.001$ ).

Parameter	EAV		SAV	
	Floc	RAS	Floc	RAS
Depth (cm)	4.7 $\pm$ 0.6 <sub>b</sub>	2.9 $\pm$ 0.4 <sub>b</sub>	7.6 $\pm$ 0.5 <sub>a</sub>	3.8 $\pm$ 0.4 <sub>b</sub>
BD (mg kg <sup>-1</sup> )***	0.043 $\pm$ 0.005 <sub>c</sub>	0.075 $\pm$ 0.005 <sub>c</sub>	0.151 $\pm$ 0.011 <sub>b</sub>	0.261 $\pm$ 0.028 <sub>a</sub>
LOI (%)***	72 $\pm$ 4 <sub>b</sub>	81 $\pm$ 2 <sub>a</sub>	20 $\pm$ 2 <sub>d</sub>	28 $\pm$ 3 <sub>c</sub>
TC (g kg <sup>-1</sup> )***	405 $\pm$ 19 <sub>b</sub>	445 $\pm$ 10 <sub>a</sub>	188 $\pm$ 8 <sub>c</sub>	224 $\pm$ 15 <sub>c</sub>
TN (g kg <sup>-1</sup> )***	33 $\pm$ 1 <sub>a</sub>	31 $\pm$ 1 <sub>a</sub>	11 $\pm$ 1 <sub>b</sub>	12 $\pm$ 1 <sub>b</sub>
TP (mg kg <sup>-1</sup> )***	1704 $\pm$ 151 <sub>a</sub>	1096 $\pm$ 58 <sub>b</sub>	683 $\pm$ 83 <sub>c</sub>	604 $\pm$ 62 <sub>c</sub>
HCl-Ca (g kg <sup>-1</sup> ) ***	104 $\pm$ 18 <sub>b</sub>	68 $\pm$ 9 <sub>b</sub>	318 $\pm$ 12 <sub>a</sub>	283 $\pm$ 13 <sub>a</sub>
HCl-Mg (g kg <sup>-1</sup> ) ***	4.8 $\pm$ 0.3 <sub>c</sub>	3.9 $\pm$ 0.2 <sub>d</sub>	9.3 $\pm$ 0.3 <sub>a</sub>	8.5 $\pm$ 0.2 <sub>b</sub>
HCl-Al (mg kg <sup>-1</sup> ) NS	186 $\pm$ 38 <sub>c</sub>	277 $\pm$ 39 <sub>ab</sub>	190 $\pm$ 40 <sub>bc</sub>	422 $\pm$ 46 <sub>a</sub>
HCl-Fe (mg kg <sup>-1</sup> ) **	181 $\pm$ 21 <sub>a</sub>	171 $\pm$ 14 <sub>a</sub>	90 $\pm$ 20 <sub>b</sub>	124 $\pm$ 16 <sub>ab</sub>
TCa (g kg <sup>-1</sup> )***	103 $\pm$ 18 <sub>c</sub>	71 $\pm$ 10 <sub>d</sub>	294 $\pm$ 8 <sub>a</sub>	263 $\pm$ 11 <sub>b</sub>
TMg (g kg <sup>-1</sup> )***	5.3 $\pm$ 0.4 <sub>b</sub>	4.3 $\pm$ 0.3 <sub>c</sub>	8.9 $\pm$ 0.2 <sub>a</sub>	8.3 $\pm$ 0.2 <sub>a</sub>
TAl (mg kg <sup>-1</sup> ) NS	722 $\pm$ 210 <sub>ab</sub>	802 $\pm$ 175 <sub>ab</sub>	681 $\pm$ 187 <sub>b</sub>	1191 $\pm$ 172 <sub>a</sub>
TFe (mg kg <sup>-1</sup> ) NS	1083 $\pm$ 246	1495 $\pm$ 231	841 $\pm$ 212	1444 $\pm$ 173

**Table 3**

Concentration of phosphorus fractions in pre-STA soils from sampling stations in STA-2. Data are presented in the form of mean  $\pm$  standard error ( $n = 11$ ). Vegetation and depth are two factors included in the two-way ANOVA. Values not connected by the same letter for each parameter (4 values in the same row) are significantly different (Tukey's test,  $\alpha = 0.05$ ). The level of significant differences between EAV and SAV is denoted by the asterisks following each parameter (NS: not significantly different; \* $P < 0.05$ ; \*\* $P < 0.01$ ; \*\*\* $P < 0.001$ ).

Parameter	EAV		SAV	
	Pre-STA 1	Pre-STA 2	Pre-STA 1	Pre-STA 2
Depth (cm)	5.0	13.8 $\pm$ 0.4	5.0	12.2 $\pm$ 0.9
BD (mg kg <sup>-1</sup> )	0.163	0.169	0.307	0.304
	$\pm$ 0.009 <sub>b</sub>	$\pm$ 0.006 <sub>b</sub>	$\pm$ 0.01 <sub>a</sub>	$\pm$ 0.012 <sub>a</sub>
LOI (%)	85.4 $\pm$ 0.6 <sub>a</sub>	85.8 $\pm$ 0.3 <sub>a</sub>	79.3 $\pm$ 1.1 <sub>b</sub>	82.4 $\pm$ 1.8 <sub>ab</sub>
TC (g kg <sup>-1</sup> )	480 $\pm$ 3 <sub>ab</sub>	502 $\pm$ 2 <sub>a</sub>	475 $\pm$ 5 <sub>b</sub>	483 $\pm$ 12 <sub>ab</sub>
TN (g kg <sup>-1</sup> )	31 $\pm$ 0.5 <sub>a</sub>	32 $\pm$ 0.5 <sub>a</sub>	28 $\pm$ 1 <sub>b</sub>	30 $\pm$ 1 <sub>ab</sub>
TP (mg kg <sup>-1</sup> )	406 $\pm$ 21 <sub>a</sub>	226 $\pm$ 10 <sub>b</sub>	407 $\pm$ 20 <sub>a</sub>	389 $\pm$ 21 <sub>a</sub>
Labile-Pi (mg kg <sup>-1</sup> )	12 $\pm$ 1 <sub>a</sub> (3)	13 $\pm$ 1 <sub>a</sub> (6)	15 $\pm$ 2 <sub>a</sub> (4)	15 $\pm$ 2 <sub>a</sub> (4)
Labile-Po (mg kg <sup>-1</sup> )	6 $\pm$ 2 <sub>a</sub> (1)	3 $\pm$ 1 <sub>a</sub> (1)	4 $\pm$ 1 <sub>a</sub> (1)	5 $\pm$ 1 <sub>a</sub> (1)
MBP (mg kg <sup>-1</sup> )	17 $\pm$ 2 <sub>a</sub> (4)	15 $\pm$ 2 <sub>a</sub> (7)	7 $\pm$ 2 <sub>b</sub> (2)	13 $\pm$ 3 <sub>a</sub> (3)
HCl-Pi (mg kg <sup>-1</sup> )	42 $\pm$ 3 <sub>b</sub> (10)	16 $\pm$ 1 <sub>b</sub> (7)	106 $\pm$ 19 <sub>a</sub> (26)	135 $\pm$ 25 <sub>a</sub> (35)
HCl-Po (mg kg <sup>-1</sup> )	25 $\pm$ 2 <sub>ab</sub> (6)	14 $\pm$ 1 <sub>c</sub> (6)	34 $\pm$ 6 <sub>a</sub> (8)	25 $\pm$ 4 <sub>bc</sub> (6)
FA-Po (mg kg <sup>-1</sup> )	74 $\pm$ 5 <sub>a</sub> (18)	47 $\pm$ 4 <sub>b</sub> (21)	76 $\pm$ 9 <sub>a</sub> (19)	79 $\pm$ 9 <sub>a</sub> (20)
HA-Po (mg kg <sup>-1</sup> )	105 $\pm$ 10 <sub>a</sub> (26)	65 $\pm$ 8 <sub>b</sub> (29)	59 $\pm$ 7 <sub>b</sub> (14)	46 $\pm$ 8 <sub>b</sub> (12)
NRP (mg kg <sup>-1</sup> )	62 $\pm$ 4 <sub>a</sub> (15)	27 $\pm$ 2 <sub>b</sub> (12)	34 $\pm$ 3 <sub>b</sub> (8)	31 $\pm$ 2 <sub>a</sub> (8)
HCl-Ca (g kg <sup>-1</sup> )	45 $\pm$ 2 <sub>b</sub>	44 $\pm$ 1 <sub>b</sub>	68 $\pm$ 4 <sub>a</sub>	44 $\pm$ 1 <sub>b</sub>
HCl-Mg (g kg <sup>-1</sup> )	4.3 $\pm$ 0.1 <sub>c</sub>	4.7 $\pm$ 0.1 <sub>ab</sub>	5.3 $\pm$ 0.2 <sub>a</sub>	4.6 $\pm$ 0.2 <sub>bc</sub>
HCl-Al (g kg <sup>-1</sup> )	1 $\pm$ 0.1 <sub>b</sub>	1.4 $\pm$ 0.1 <sub>a</sub>	1.4 $\pm$ 0.1 <sub>ab</sub>	1.7 $\pm$ 0.3 <sub>a</sub>
HCl-Fe (mg kg <sup>-1</sup> )	136 $\pm$ 9 <sub>b</sub>	167 $\pm$ 17 <sub>b</sub>	170 $\pm$ 11 <sub>b</sub>	641 $\pm$ 96 <sub>a</sub>
TCa (g kg <sup>-1</sup> )*	46 $\pm$ 2 <sub>b</sub>	44 $\pm$ 1 <sub>b</sub>	65 $\pm$ 4 <sub>a</sub>	43 $\pm$ 2 <sub>b</sub>
TMg (g kg <sup>-1</sup> )*	4.4 $\pm$ 0.1 <sub>b</sub>	4.9 $\pm$ 0.1 <sub>ab</sub>	5.2 $\pm$ 0.2 <sub>a</sub>	5.3 $\pm$ 0.3 <sub>a</sub>
TAI (g kg <sup>-1</sup> ) NS	1.8 $\pm$ 0.1	2.2 $\pm$ 0.1	2.0 $\pm$ 0.2	3.4 $\pm$ 1.1
TFe (g kg <sup>-1</sup> )*	2.0 $\pm$ 0.3	1.9 $\pm$ 0.2	2.4 $\pm$ 0.1	3.0 $\pm$ 0.4

flow-path while labile Pi accounted for up to 30% of total P in SAV at the inflow to mid region of the FW and decreased with distance downstream (Fig. 5a). Labile Pi in pre-STA soils of both EAV and SAV ranged from 3 to 6% of total P (Table 3).

Highly reactive organic P (HRPo) that includes both labile Po and MBP was significantly higher in EAV than SAV in floc and RAS ( $P < 0.05$ , Fig. 4). Labile Po in floc was higher at the inflow site compared to midflow and outflow locations in both EAV and SAV FWs (Fig. 4). Labile Po in RAS showed no significant differences among inflow, midflow and outflow stations of the EAV FW but decreased significantly from inflow to outflow in the SAV FW (Fig. 4). Microbial biomass P was higher in floc than RAS in EAV ( $P < 0.05$ ) but showed no difference in SAV FW

(Fig. 4). In EAV, HRPo accounted for approximately 10–40% and 5–20% of total P in floc and RAS, respectively and increased with distance from inflow (Fig. 5a). In SAV, HRPo accounted for approximately 5–30% and 5–10% of total P in floc and RAS, respectively (Fig. 5a). The HRPo in pre-STA soils ranged from 5 to 8% of total P in EAV and <4% of total P in SAV (Table 3).

### 3.2.2. Reactive phosphorus [RP]

Reactive inorganic P (RPI) (acid extractable, HCl-Pi) in floc and RAS showed no distinct gradient along the flow-path in EAV, but in the SAV FW RPI decreased with distance from inflow (Figs. 4 and 5b). Reactive Pi accounted for 18–29% of the total P in floc and RAS of the EAV and 23–55% of the total P in floc and RAS of the SAV (Fig. 5b). The RPI in pre-STA soils ranged from 7 to 10% of total P in EAV and 26 to 35% of total P in SAV (Table 3).

Reactive Po includes both acid and alkali extractable organic P (RPo). Reactive Po ranged from 24 to 44% and 39 to 49% of total P in floc and RAS of EAV, respectively (Fig. 5b). In SAV, RPo ranged from 15 to 37% of total P in floc and 8 to 42% of total P in RAS and increased with distance from inflow (Fig. 5b). Reactive Po expressed as a fraction of total P showed no consistent trend along the EAV flow-path, while in the SAV system, an increase in this pool was noted with distance from inflow (Fig. 5b). The RPo in pre-STA soils ranged from 24 to 27% of total P in EAV and SAV (Table 3). All forms of RPo including HCl-Po, fulvic acid (FA-Po), and humic acid (HA-Po) showed significant differences between EAV and SAV ( $P < 0.05$ , Fig. 4). In EAV, both FA-Po and HCl-Po showed decreasing trend with distance from inflow in EAV, while in SAV no significant trend with distance was observed (Fig. 4). However, HA-Po decreased with distance from inflow in floc, but increased with distance in RAS (Fig. 4).

### 3.2.3. Non-reactive phosphorus (NRP)

In the EAV system, NRP accounted for 7–24% of TP in floc and 15–25% of TP in RAS compared to 6–15% and 13 to 27% in floc and RAS from SAV FW, respectively (Fig. 5b). Although NRP concentrations in floc and RAS were higher in EAV than SAV, NRP in both systems significantly decreased ( $P < 0.05$ , Fig. 4) along the flow-path.

### 3.2.4. Mineralogy of soils

The dominant crystalline inorganic component in RAS samples from each of the six benchmark sites was calcium carbonate ( $\text{CaCO}_3$ ), based on XRD (data not shown). The only distinction between the EAV and SAV samples was the raised baseline of the EAV XRD plot, particularly at the outflow, indicative of abundant amorphous materials (e.g., organic matter, biogenic Si). Calcite was the prevalent mineral,

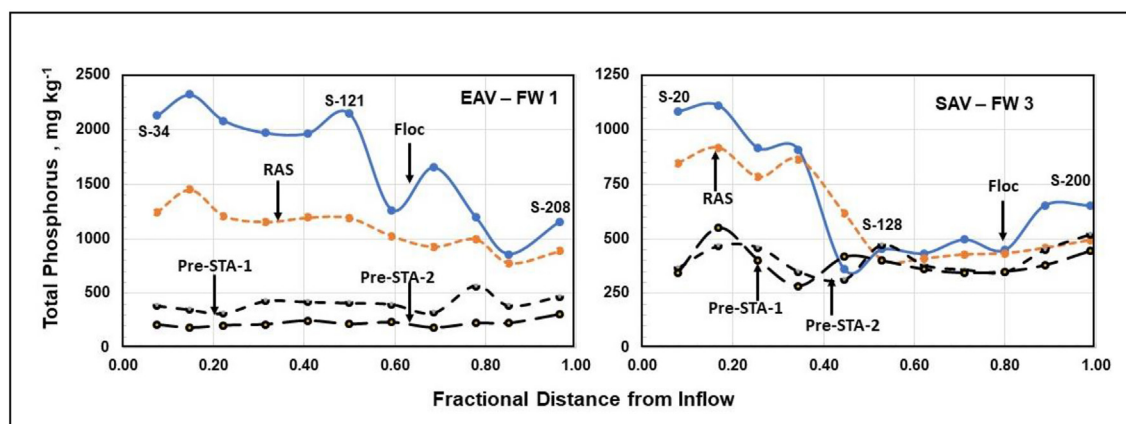
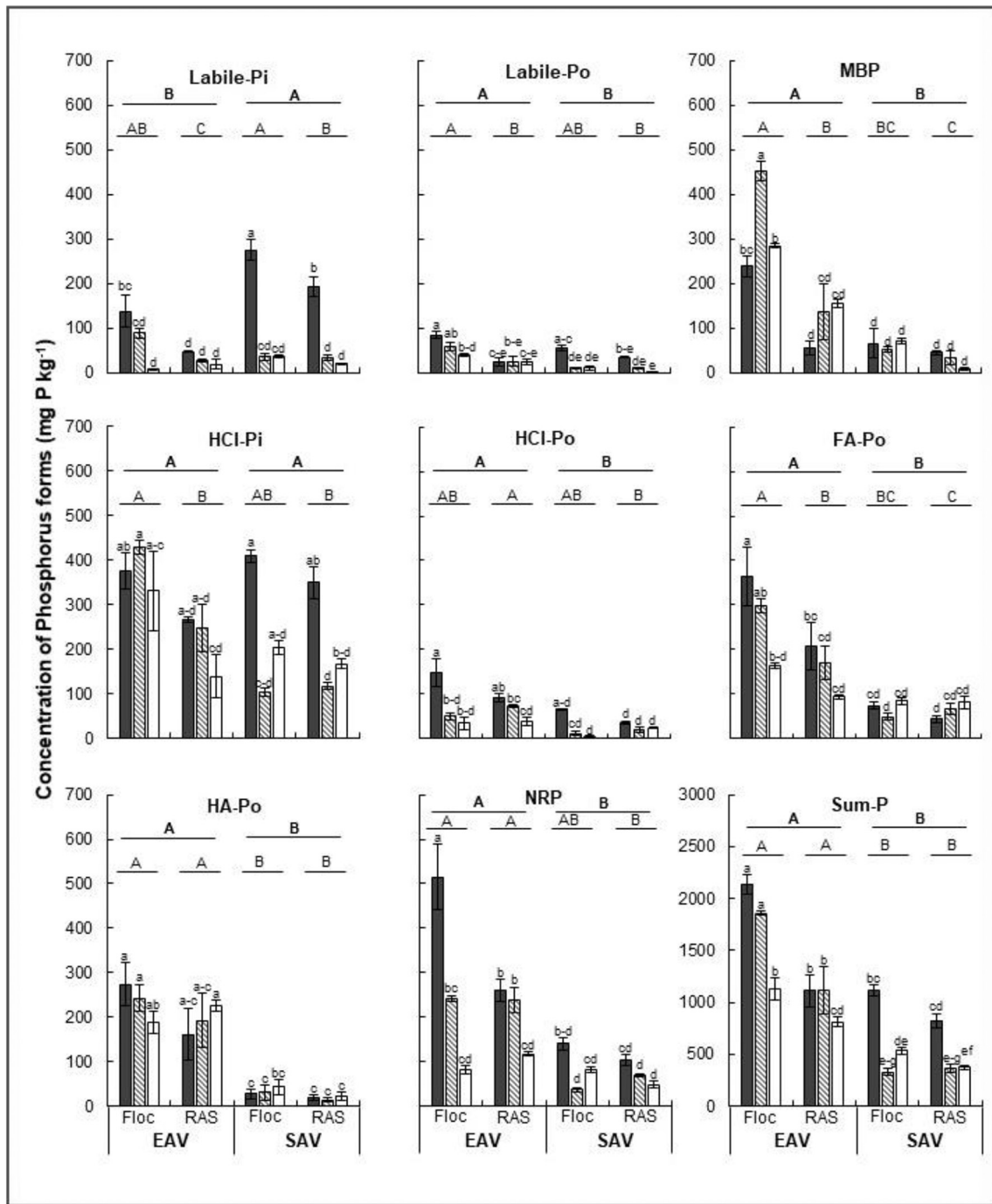


Fig. 3. Total phosphorus concentration in floc, RAS, and pre-STA soils collected along the distance from inflow of FW 1 (EAV) and FW 3 (SAV).



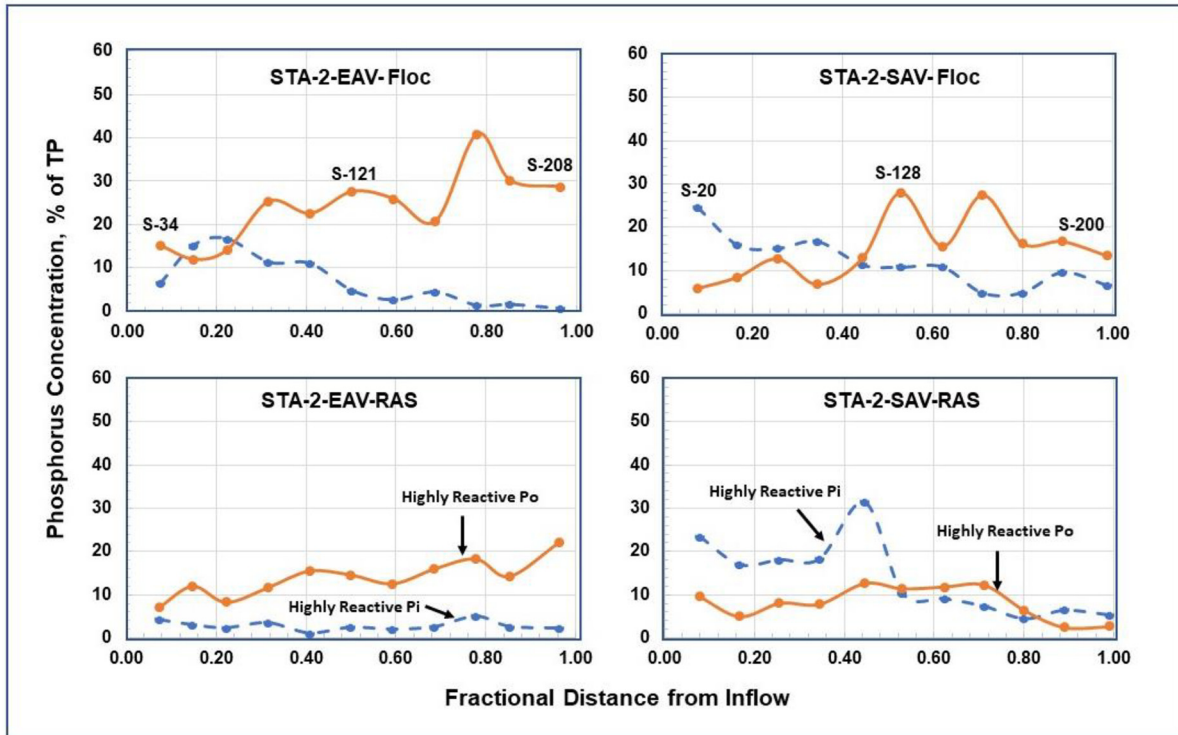
**Fig. 4.** Concentration of phosphorus forms in floc and RAS from benchmark stations in STA-2. Data are mean  $\pm$  standard error ( $n = 3$ ). Values not connected by the same letter are significantly different between vegetation types, distance or depth (Tukey's test,  $\alpha = 0.05$ ).

but aragonite (another mineral form of  $\text{CaCO}_3$ ) was also detected in five of the six samples. Quartz ( $\text{SiO}_2$ ), dolomite [ $\text{CaMg}(\text{CO}_3)_2$ ], and palygorskite [ $(\text{Mg}, \text{Al})_5(\text{Si}, \text{Al})_8\text{O}_{20}(\text{OH})_2 \cdot 8\text{H}_2\text{O}$ ] were tentatively identified as minor components in some samples. This mineralogy is consistent with pH values and with high Ca concentrations and relatively high Mg concentrations in the samples, as extracted by 1 M HCl (Table 2). No phosphate minerals were detected by XRD, but SEM-EDS elemental dot maps and point spectra for two EAV RAS samples showed elevated P to be mainly restricted to small, scattered Ca-P particles (Fig. 6) whereas Ca was ubiquitously distributed due to the dominance of  $\text{CaCO}_3$  in the samples.

### 3.2.5. Phosphorus forms-NMR spectroscopy

Total P concentrations in the single-step NaOH-EDTA extract for NMR analysis ranged from 386 to 2127  $\text{mg kg}^{-1}$  in EAV and 365 to 1244  $\text{mg kg}^{-1}$  in SAV samples, with lower values in pre-STA soils and higher values in floc (Table 4a, Fig. 3). This alkaline extraction accounted for approximately 46 and 60% of total P in EAV and SAV, respectively. NMR spectra of these extracts identified broad range of P forms, including phosphomonoesters, phosphodiester, and pyrophosphates (Fig. 7). In EAV samples, phosphomonoesters accounted for 14 to 25% of total P in floc and RAS and 20–28% in pre-STA soils, as compared to 17 to 28% in floc and RAS, and

a



b

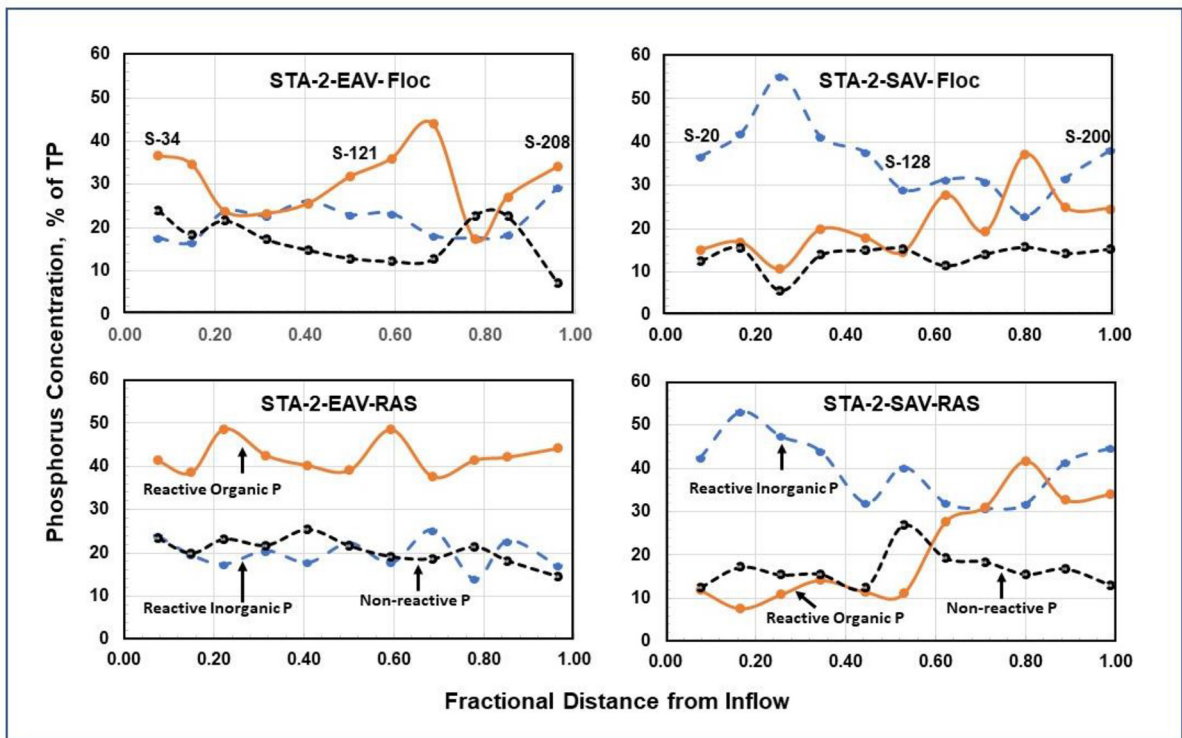


**Fig. 5.** a. Concentration of highly reactive phosphorus (HRP-labile organic P including microbial biomass P and labile inorganic P) expressed as percent of total P in the floc and RAS from FW 1 (EAV) and FW 3 (SAV). b. Concentration of reactive organic P (RPo), reactive inorganic P (RPI), and non-reactive P (NRP) expressed as percent of total P in the floc and RAS soil sections from FW 1 (EAV) and FW 3 (SAV).

30–45% in pre-STA soils of SAV (Table 4a). In EAV, phosphodiester accounted for 11 to 19% of total P in floc and RAS, and 15–28% in pre-STA soils, as compared to 5 to 18% in floc and RAS and 6–10%

in pre-STA soils of SAV (Table 4a). The ratio of monoester P to diester P ranged from 0.85 to 1.2 in EAV floc and RAS, as compared to 1.2 to 3.4 in SAV floc and RAS (Table 4a).

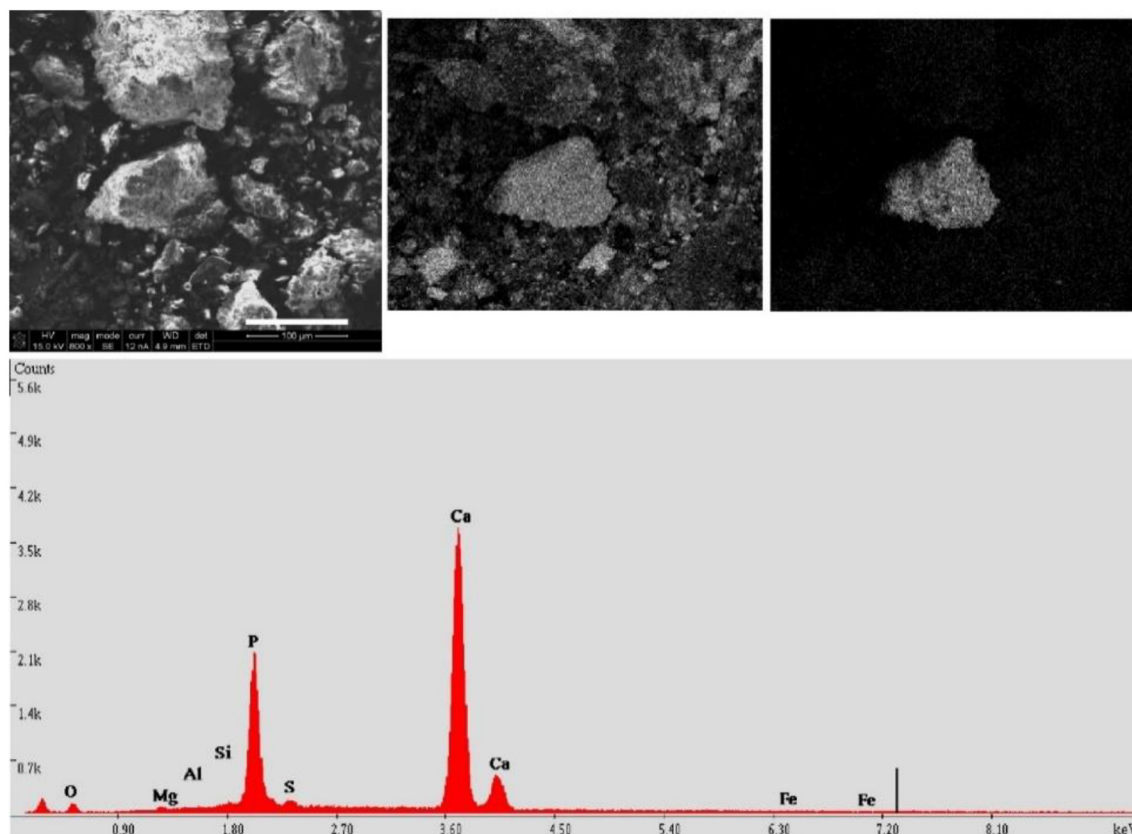


**Fig. 6.** Upper left: Secondary electron image of P-rich particle in EAV RAS inflow sample (center of frame; scale bar = 100  $\mu\text{m}$ ). Upper middle: Ca dot map. Upper right: P dot map. Lower: Spectrum of the particle collected in spot mode (focused exclusively on particle). Other such associations were documented in this sample and another EAV RAS sample. The Ca-P association was not diffuse but rather was highly localized in particles consistent with a discrete mineral phase. Calcium is not localized but rather occurs ubiquitously throughout the sample due to the dominance of calcite (as confirmed by XRD).

In the EAV system, the labile Po and MBP pools were positively correlated with phosphomonoesters and phosphodiester, which were also significantly correlated with operationally defined RPo pools, including HCl-Po, FA-Po, and HA-Po ( $P < 0.001$ , Table 4b). However, phosphomonoesters correlated with only HCl-Po ( $P < 0.05$ ), and phosphodiester correlated with HRP and NRP and in SAV FW ( $P < 0.05$ ).

### 3.3. Phosphorus storage

At the time of this study, both FWs had been in full operation for 14 years (2002 to 2016) thus P storage in floc and RAS reported in our study represents the effects of a long-term operational period. Both HRP and RP pools were significantly influenced by vegetation, with

**Table 4a**

Organic P forms ( $\text{mg kg}^{-1}$ ) determined by NMR in floc, RAS, and pre-STA soil samples from inflow, midflow and outflow sites of STA-2 FW1 and FW3. ND = Not detected. Values in parenthesis represent percent of total P.

FW/Location	Depth	Total P	Phosphorus ( $\text{mg kg}^{-1}$ ) (% total P)					Ratio: monoester P/diester P
			NaOH-TP	Ortho-P	Phosphomonoesters	Phosphodiester	Pyrophosphate	
FW-1 (EAV) Inflow	Floc	2127	855 (40)	165 (8)	351 (17)	325 (15)	14 (1)	1.08
	RAS	1244	702 (56)	141 (11)	312 (44)	237 (19)	12 (1)	1.32
	Pre-STA1	386	190 (49)	41 (11)	102 (26)	45 (12)	3 (1)	2.27
Midflow	Floc	2186	1091 (46)	500 (23)	315 (14)	249 (11)	27 (1)	1.27
	RAS	946	481 (51)	176 (19)	135 (14)	159 (14)	11 (1)	0.85
	Pre-STA1	316	194 (61)	91 (29)	64 (20)	39 (12)	ND	1.64
Outflow	Floc	1555	761 (49)	225 (14)	250 (16)	239 (15)	48 (3)	1.05
	RAS	887	566 (64)	165 (19)	203 (23)	170 (19)	27 (3)	1.19
	Pre-STA1	469	255 (54)	82 (17)	131 (28)	38 (8)	5 (1)	3.45
FW-3 (SAV) Inflow	Floc	1083	508 (47)	224 (21)	193 (18)	84 (8)	7 (1)	2.30
	RAS	847	347 (41)	146 (17)	155 (18)	46 (5)	ND	3.37
	Pre-STA1	365	302 (83)	116 (32)	150 (41)	36 (10)	ND	4.17
Midflow	Floc	434	259 (60)	92 (21)	86 (20)	75 (17)	6 (1)	1.15
	RAS	409	189 (46)	80 (20)	70 (17)	38 (9)	ND	1.84
	Pre-STA1	379	237 (63)	88 (23)	114 (30)	36 (9)	ND	3.17
Outflow	Floc	652	362 (56)	64 (10)	182 (28)	116 (18)	ND	1.57
	RAS	493	215 (44)	18 (4)	140 (28)	57 (12)	ND	2.46
	Pre-STA1	519	330 (64)	66 (13)	233 (45)	31 (6)	ND	7.52

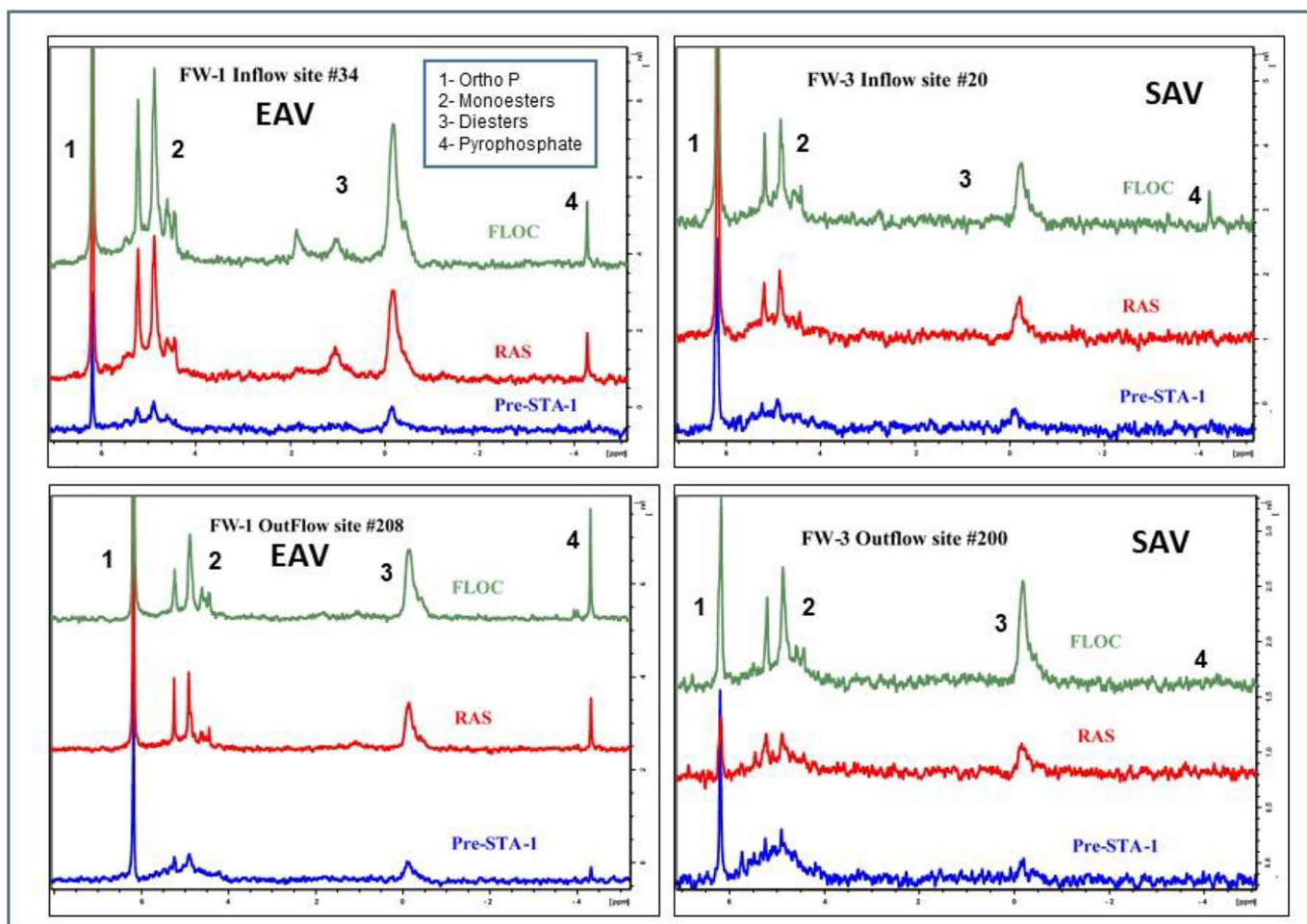


Fig. 7. Solution  $^{31}\text{P}$  nuclear magnetic resonance spectra from floc and RAS samples of EAV and SAV flow-ways.

high rates of P accretion in SAV as compared to EAV ( $P < 0.05$ , Table 5, Fig. 8). In both EAV and SAV, P storage was high in floc and RAS near the inflow and decreased along the flow-path (Fig. 8). Average total P storage in floc and RAS (combined) along the flow-path was  $5 \text{ g P m}^{-2}$  (57% in floc and 43% in RAS) in EAV and  $16 \text{ g P m}^{-2}$  (56% in floc and 44% in RAS) in SAV FWs (Table 5). Phosphorus loading increased the proportion of P stored as inorganic P in SAV systems and as organic P in EAV systems. The mass ratio of TPi/TPo in floc and RAS of EAV system is 0.5 and decreased with distance from inflow, suggesting accumulation of organic P, while high ratios of up to 2.5 in SAV system suggest inorganic P accumulation in the floc and RAS (Fig. 8).

Highly reactive P forms in the floc accounted for approximately 30% of the stored P in both EAV and SAV FWs, while in the RAS layer, HRP

accounted for 16% of P stored in EAV and 28% in SAV (Table 5). The RP pool accounted for a larger proportion of soil P storage with 51 and 64% of the total P stored in EAV and SAV systems, respectively. NRP pool accounted for 13 to 15% of stored P in SAV and 18 to 20% of stored P in EAV (Table 5). Storage of HRP and RP pools in pre-STA soils accounted for approximately 80 to 88% of the total P stored in EAV and 92% of stored P in SAV (Table 5).

Phosphorus storage in soil was dominated by organic P (HRPo + RPo) in the EAV system and by inorganic P (HRPi + RPi) in the SAV system (Fig. 8). In EAV floc, approximately 25 to 52% of total P was inorganic and 48 to 75% was organic. In EAV RAS, 23 to 38% was inorganic and 62 to 77% organic. In SAV floc, approximately 33 to 75% of total P was present in inorganic P pool and 25 to 67% in organic P

Table 4b

Spearman's  $\rho$  value showing correlations between phosphomonoesters and phosphodiester and organic P forms organic P forms in floc, RAS, and pre-STA soils (0–5 cm) from benchmark locations in STA-2 FW 1 and 3. Significance level: \* $P < 0.05$ ; \*\* $P < 0.01$ ; and \*\*\* $P < 0.001$  level; NS = not significant.

Organic P forms	EAV			SAV	
	Phosphomonoesters	Phosphodiester	Pyrophosphate	Phosphomonoesters	Phosphodiester
Highly reactive Po					
Labile organic P	0.92***	0.90***	0.65**	0.05 NS	0.49*
Microbial biomass P	0.83***	0.85***	0.90***	0.02 NS	0.83***
Reactive Po					
Acid extractable Po	0.80***	0.73***	0.28 NS	0.52*	−0.44 NS
Alkali extractable – FA-P	0.95***	0.87***	0.45 NS	0.22 NS	−0.14 NS
Alkali extractable – HA-P	0.78***	0.73***	0.59**	0.30 NS	−0.40 NS
Non-reactive P	0.87***	0.80***	0.36 NS	0.30 NS	0.71***

**Table 5**  
Total phosphorus storage in the floc, RAS, and pre-STA soils of EAV and SAV flow-ways. Phosphorus pools: HRP – highly reactive P; RP – moderately reactive P; NRP – non-reactive P. Data are mean  $\pm$  standard error (n = 11). Values not connected by the same letter are significantly different between vegetation types or depth (Tukey's test,  $\alpha = 0.05$ ). Values in parenthesis represent percent of total P storage. #Phosphorus storage calculated based on difference between inflow and outflow P loads.

Flow-way	Soil layers	g P m <sup>-2</sup> (% of total P storage)			Total P storage	Total P retention# [14 years]
		HRP	RP	NRP		
EAV	Floc	0.84 $\pm$ 0.10 <sub>b</sub> (30)	1.43 $\pm$ 0.18 <sub>b</sub> (51)	0.49 $\pm$ 0.08 (18)	2.8 $\pm$ 0.3 <sub>b</sub>	10.9
	RAS	0.33 $\pm$ 0.05 <sub>b</sub> (16)	1.35 $\pm$ 0.27 <sub>b</sub> (64)	0.45 $\pm$ 0.10 (21)	2.1 $\pm$ 0.4 <sub>b</sub>	
	Total	1.17 (24)	2.78 (57)	0.94 (19)	4.9	
SAV	Floc	2.64 $\pm$ 0.61 <sub>a</sub> (29)	5.21 $\pm$ 1.32 <sub>a</sub> (58)	1.14 $\pm$ 0.27 (13)	9.0 $\pm$ 2.1 <sub>a</sub>	14.8
	RAS	1.86 $\pm$ 0.60 <sub>ab</sub> (28)	3.77 $\pm$ 0.97 <sub>ab</sub> (56)	1.03 $\pm$ 0.27 (15)	6.7 $\pm$ 1.8 <sub>ab</sub>	
	Total	4.50 (29)	8.98 (57)	2.17 (14)	15.7	

pool, while in RAS approximately 47 to 85% was present in inorganic P pool and 15 to 53% in organic P pool. In both systems, a large portion of accreted P was found near the inflow region of both FWs and decreased with distance downstream (Fig. 8). On annual basis, total P accretion rate in floc and RAS was estimated to be 0.35 g P m<sup>-2</sup> y<sup>-1</sup> in EAV as compared to 1.12 g P m<sup>-2</sup> y<sup>-1</sup> in SAV (Table 5).

### 3.4. Relationship between phosphorus forms and biogeochemical properties of soils

The principal component analysis was applied on variables including concentrations of P fractions and other selected biogeochemical properties, which showed a clear separation between EAV and SAV FWs in the score plot (Fig. 9). The score plot (left) of PCA also indicated a clear separation between pre-STA and new accreted soils in both EAV (along the empty arrow) and SAV (along the solid grey arrow) FWs. In EAV FW, floc and RAS were mainly separated by organic P variables, including total labile-Po (MBC and labile Po), HCl-Po, FA-Po, HA-Po, NRP, and BD from pre-STA soils, with higher organic and residual P concentrations

and lower BD in newer layers (loading plot, right). In SAV FW, higher inorganic P (labile Pi and HCl-Pi), Ca and Mg concentrations and pH distinguished floc and RAS from pre-STA soil with relatively higher TC, TN, Fe and Al content (loading plot, right). Meanwhile, the separation between EAV and SAV FWs was more evident in newer layers. The correlations between P forms and acid extractable metals in floc and RAS were different between EAV and SAV FWs (Table 6).

## 4. Discussion

### 4.1. Phosphorus enrichment in recently accreted material (floc and RAS)

Phosphorus concentrations (expressed on dry weight basis, mg kg<sup>-1</sup>) in floc and RAS were significantly higher in EAV than SAV systems (Fig. 3). This distinct difference between two vegetation types was due to accretion of predominantly organic matter in EAV, while accretion of mineral matter supported by the production of CaCO<sub>3</sub> and other associated metals in SAV, resulting in significantly lower bulk density of accreted material in EAV than SAV (Table 2). Although P

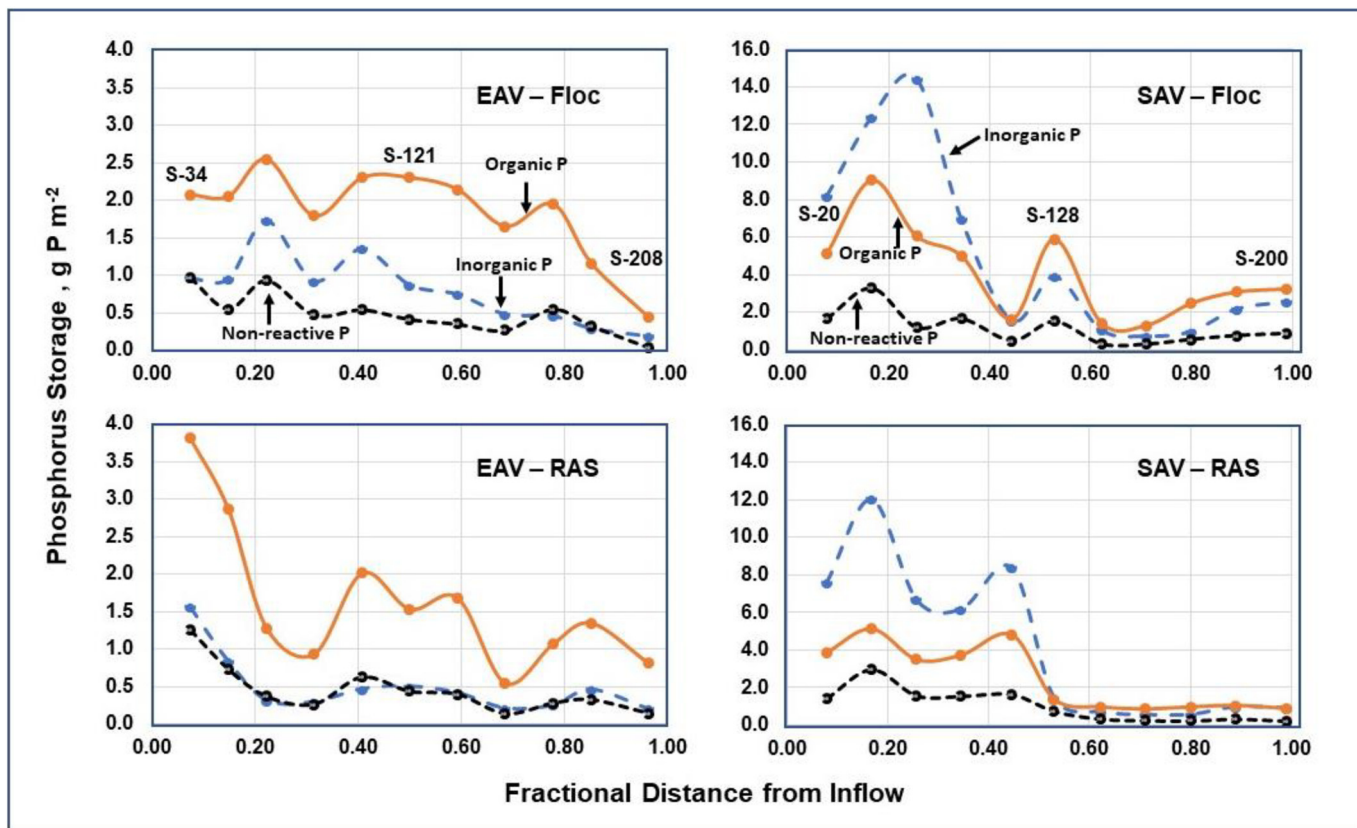


**Fig. 8.** Inorganic and organic P storage in EAV and SAV systems as a function of distance from inflow.

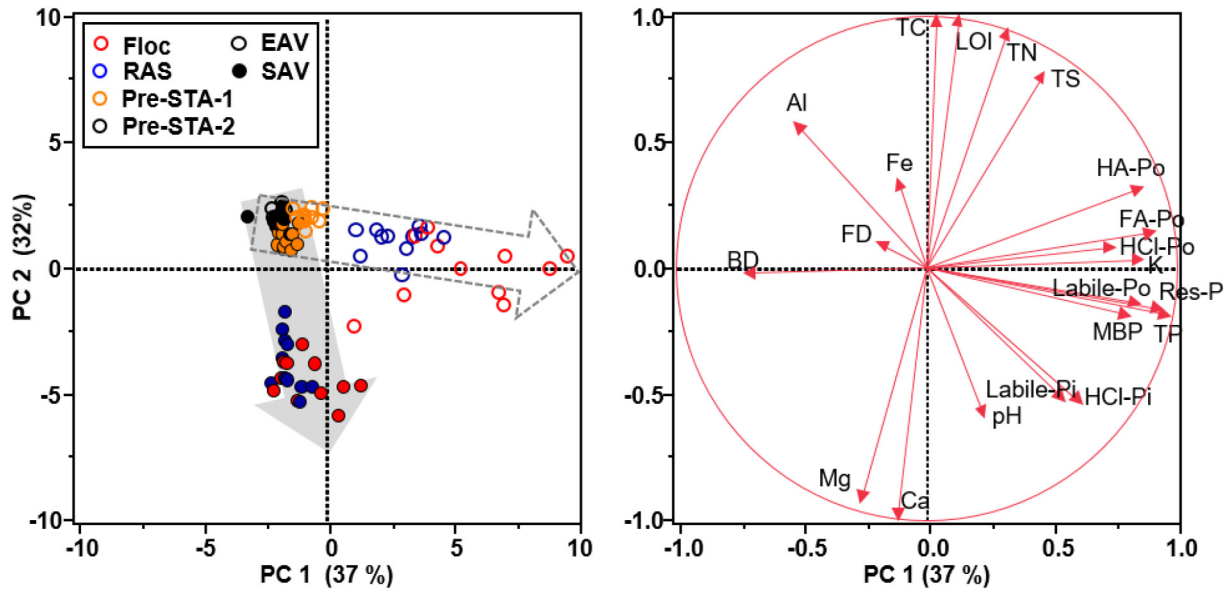


Fig. 9. Multivariate analysis of phosphorus forms and associated biogeochemical properties in EAV and SAV flow-ways of STA-2.

concentrations of floc and RAS were lower in SAV than EAV, the amount of P stored per unit area was significantly higher in SAV than EAV (Table 5). Similar patterns were also noted in the Everglades and other wetland ecosystems (DeBusk et al., 1994; Bhomia et al., 2015; Morris et al., 2016; Newman et al., 2017; Qualls and Heyvaert, 2017). Our study showed significant P enrichment in floc and soils in the first half of flow-path in both EAV and SAV systems. Similar to our study, long-term P loading to wetlands results in distinct spatial and vertical P gradients in floc and soils with high P concentrations and storages in areas closer to inflow and decreasing along the flow-path towards the outflow (DeBusk et al., 1994; Bhomia et al., 2015; Newman et al., 2017).

In upstream areas of FWs, P enrichment supported high P levels in highly and moderately reactive P pools in floc and soils which suggests surplus P conditions that can potentially support flux into the water column. Both FWs were effective in retaining approximately 80 and 85% of P loaded to SAV and EAV systems of STA-2, respectively (Zhao and Piccone, 2020). In EAV FW, approximately 45% of the P retained was recovered in floc and RAS and remaining was unaccounted for and possibly retained in the above and below ground biomass and incorporated into subsurface soils. In WCA-2a, Miao and Sklar (1998) reported standing crop EAV-Typha biomass of 1240 g m<sup>-2</sup> with 60% accounted for aboveground and 40% belowground biomass. Phosphorus storage in Typha biomass (above and belowground biomass) in P-enriched sites of WCA-2a was reported to be 4 to 5 g P m<sup>-2</sup> (Miao and Sklar, 1998). Other studies have shown approximately 14 to 45% of added P was

recovered in above ground biomass of cattails (Weng et al., 2006; Kadlec and Bevis, 2009). In SAV FW, all of the P retained was recovered in floc and soils suggesting P retention in plants was not significant. Depending on vegetation types and source of inflow water, P stored in floc and soils can be present in organic and inorganic forms and its reactivity and physico-chemical properties influence the mobility of P from soils to overlying water column and potential transport downstream (Andersen et al., 2017; Reddy et al., 1998; Yang and Post, 2011).

4.2. Soil phosphorus forms

4.2.1. Highly and moderately reactive P

In our study, we focused on highly reactive P (labile Pi, labile Po, and MBP) and moderately reactive P (acid extractable Pi, and acid and alkali extractable Po). Relative proportion of these P forms were regulated predominantly by biotic processes in EAV FW and coupled biotic and abiotic processes in SAV FW. Highly reactive P is bioavailable on short time scales with high turnover rates (Huang et al., 2015; Maharjan et al., 2018; Oberson and Joner, 2005; Reddy et al., 2005; Torres et al., 2017, 2014). Sources of labile Pi include, porewater Pi that is in equilibrium with the Pi sorbed onto metal oxides and organic matter, and mineralization of organic P. This P pool is readily available to microbes, periphyton, and macrophytes and also regulates the P concentration of the overlying water column (Fig. 10) (Reddy et al., 2005). Highly reactive Po including both labile Po and active MBP (Fig. 2) was

Table 6

Spearman's ρ value showing correlation coefficients between phosphorus forms and acid (1 M HCl) extractable metals in floc and RAS of STA-2 (n = 22). Significance level: \*P < 0.05; \*\*P < 0.01; and \*\*\*P < 0.001 level; NS = not significant.

Phosphorus pools	EAV				SAV			
	Ca	Mg	Fe	Al	Ca	Mg	Fe	Al
MBP	0.26NS	0.46*	-0.12NS	-0.52*	0.51*	0.47*	-0.18NS	-0.6**
NaHCO <sub>3</sub> -Pi	0.25NS	0.45*	0.6**	0.16NS	0.26NS	-0.1NS	0.52*	-0.09NS
Labile Po	-0.01NS	0.31NS	-0.04NS	-0.06NS	0.34NS	0.37NS	-0.13NS	-0.45*
HCl Pi	0.19NS	0.53*	0.27NS	0.01NS	-0.01NS	-0.3NS	0.67***	0.2NS
HCl Po	-0.35NS	-0.12NS	0.43*	0.61**	-0.2NS	-0.48*	0.68***	0.3NS
NaOH FA-Po	-0.06NS	0.2NS	0.32NS	0.17NS	-0.41NS	-0.05NS	-0.11NS	0.17NS
NaOH HA-Po	-0.22NS	0.25NS	0.23NS	0.4NS	0.01NS	-0.16NS	0.06NS	-0.03NS
Residual P	0.29NS	0.51*	0.52*	0.1NS	-0.09NS	-0.12NS	0.63**	0.22NS
Total Pi	0.15NS	0.51*	0.31NS	0.07NS	0.04NS	-0.28NS	0.64**	0.15NS
Total Po	0.04NS	0.44*	0.24NS	-0.02NS	0.22NS	0.12NS	-0.01NS	-0.32NS
Total P	0.10NS	0.48*	0.35NS	0.07NS	0.09NS	-0.17NS	0.59**	0.05NS

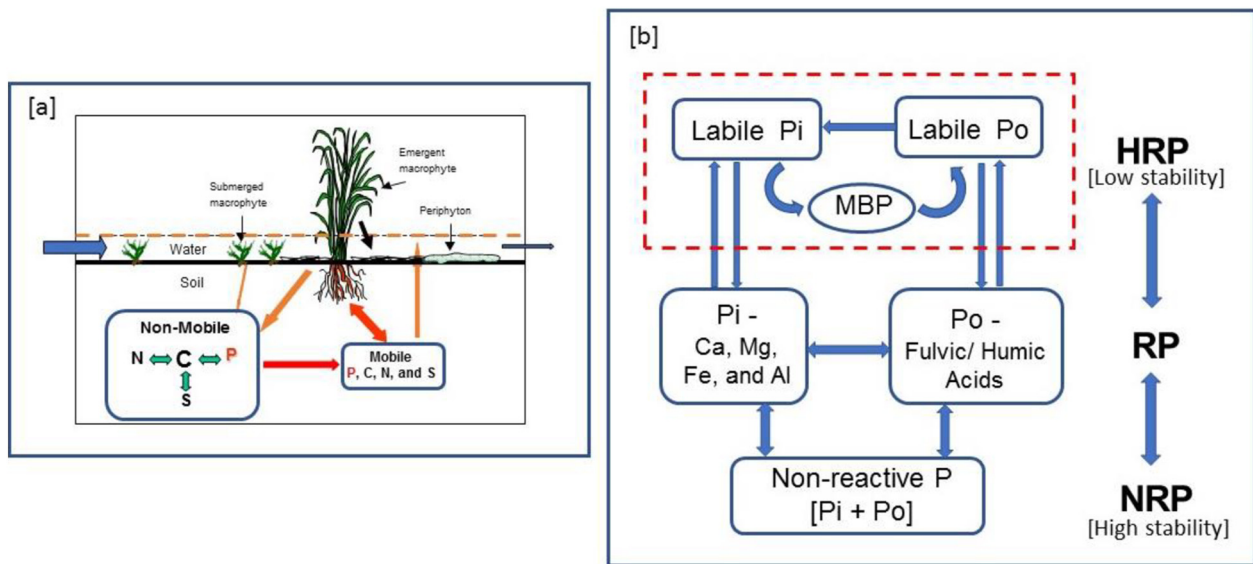


Fig. 10. [a] - Schematic showing mobile and non-mobile pools of macro-elements including phosphorus. [b] - Linkages between reactivity and stability of phosphorus pools in floc and soils.

dominated by phospho-diester such as polymeric nucleotides including DNA and RNA, but may also include other forms of organic P including phosphomonoesters (Tables 4a and 4b) (Cheesman et al., 2014; Koch et al., 2018; Turner et al., 2006; Turner and Newman, 2005).

Moderately reactive P pools includes inorganic P associated with Ca, Mg, Fe, and Al, while acid and alkali extractable P associated with phosphomonoesters and phosphodiester (Cheesman et al., 2014; Turner et al., 2006; Turner and Newman, 2005). Moderately reactive P is available at longer time scales with slow turnover rates and this pool of P potentially serves as source of or sink for bioavailable pools (Reddy et al., 2005).

In the EAV FW, organic P pools in floc and RAS contained both phosphor-monoesters and diesters (Fig. 4 and Table 4a). Organic P in the system must first undergo enzymatic hydrolysis where ester linkages (oxygen-phosphorus bonds) in both mono- and diesters are broken resulting in the release of phosphate into soil porewater (Turner et al., 2006; Turner and Newman, 2005; Watson et al., 2018). Large proportion of labile Po and MBP in HRP suggests that mineralization of organic P is likely the key process producing labile Pi in floc and RAS in EAV system. Net mineralization rates of organic P in P-enriched areas of the FW are positive resulting in net release of labile Pi (Bünemann, 2015; Reddy and DeLaune, 2008). In P-limited systems such as those in oligotrophic wetlands, any organic P mineralized is rapidly scavenged by microbes to meet their cellular requirements and growth (Noe et al., 2001; Reddy et al., 1999). Under these conditions, net mineralization rates are negative as indicated by the rapid assimilation of labile Pi into microbial biomass (Bünemann, 2015; Reddy and DeLaune, 2008; Richardson and Simpson, 2011; Zhu et al., 2018). These patterns are evident in our study as larger proportion P (expressed % of total P) in floc and soils was higher in downstream P-limited areas of both EAV and SAV systems (Fig. 5a).

Moderately reactive Po (RPO) extracted with acid (HCl-Po) and alkali (FA-Po and HA-Po) is coupled with organic matter. Phosphorus associated with the organic matter may include phospholipids, nucleic acids, inositol phosphates, glucose-6-phosphates, glycerophosphate, phosphoproteins, and polymeric organic P of high-molecular-weight compounds (Cheesman et al., 2014). RPO includes phosphomonoesters such as inositol phosphates and phosphodiester as identified by NMR (Table 4a). Although, phosphomonoesters are reactive, they are much more stable in soils than phosphodiester (Torres et al., 2017, 2014; Turner et al., 2002). Due to reactive *o*-phosphate groups, the inositol hexaphosphate (IHP) monoester is prone to strong adsorption to

humic and fulvic acid components of the stable organic matter (Celi and Barberis, 2007; Celi and Barberie, 2005; Turner et al., 2002). The decomposition of organic matter and mineralization of organic P is regulated by several factors including; nutrient load, physico-chemical environment of soil, floc and water column, and chemical composition of litter, floc, and soils. All these factors are pertinent to STAs in regulating biogeochemical processes and P mobility from high concentration zones to low concentration zones.

In the SAV FW, inorganic P dominated the P pools in both floc and RAS, with high concentrations at sites of up to <1.5 km from the inflow (Figs. 4 and 5). High concentrations of labile Pi in floc and RAS layers also suggest rapid mineralization of organic P associated with SAV detrital matter as compared to EAV (Chimney and Pietro, 2006; DeBusk and Reddy, 2005; Song et al., 2013). Inorganic P in the water column is directly in contact with SAV with its leaves coated with  $\text{CaCO}_3$  due to active photosynthesis in the water column (Pedersen et al., 2013). In addition to P uptake by biotic communities in SAV, some of the inorganic P may co-participate or occlude with  $\text{CaCO}_3$  in the water column and deposited into the floc and ultimately incorporated into RAS. The underwater photosynthetic activity of SAV creates environmental conditions (high pH, low carbon dioxide partial pressure) in the water column that favors precipitation of  $\text{CaCO}_3$  (Andersen et al., 2017; Farve et al., 2004; Pelechaty et al., 2013; Reid and Mosley, 2016; Siong et al., 2006). Lack of significant correlation between labile Pi and acid extractable Ca was probably due to high concentrations of  $\text{CaCO}_3$  which masked the relationship with P pools in SAV system. Significant correlation was noted between labile Pi and acid extractable Fe in both EAV and SAV systems ( $P < 0.01$  for EAV and  $P < 0.05$  for SAV, Table 6) suggesting possible displacement of phosphate ions from Fe-P complexes with  $\text{OH}^-$  and carboxyl ions under alkaline conditions (Reddy and DeLaune, 2008).

Reactive Pi includes Fe and Al bound P and Ca and Mg bound P present as amorphous and poorly crystalline forms and are soluble in acid and extracted with 1 M HCl (Fig. 4). A significant correlation between reactive Pi and acid extractable Fe ( $P < 0.01$ ) was observed in  $\text{CaCO}_3$  dominated SAV system and no significant relationship in EAV system (Table 6). In SAV, water column and floc conditions are ideal for  $\text{CaCO}_3$  formation and it is likely that Ca phosphate, Al phosphate, and Fe phosphate are occluded with  $\text{CaCO}_3$  and retained in floc and RAS (Pelechaty et al., 2013; Reddy and DeLaune, 2008; Siong et al., 2006).

Earlier studies in agricultural soils reported poor relationship between P retention capacity and total or active  $\text{CaCO}_3$  contents (Hamad

et al., 1992; Ryan et al., 1985; Solis and Torrent, 1989). In calcareous sediments of Lake Okeechobee, Moore and Reddy (1994) showed that Fe phosphate precipitation controls the behavior of P in surface sediments under aerobic conditions such as those noted in SAV floc and overlying water column interface, whereas Ca phosphate governs P solubility under anaerobic conditions. Lalonde et al. (2012) estimated that approximately 22% of reactive Fe is complexed with organic carbon, possibly due to co-precipitation and/or direct chelation, and process potentially involved in the preservation of organic carbon in sediments. Iron is known to be scavenged by colloids through iron-binding ligands (Boyd and Ellwood, 2010; Colombo et al., 2014). It is possible in SAV flow-way colloidal planktonic particles with encrustation of  $\text{CaCO}_3$  with coating of DOM can complex with Fe in the water column and ultimately settle into floc layer. In EAV flow-way colloidal particles may consist of particulate organic matter which can also complex with Fe and P and settle into floc layers. Iron extracted using HCl and ammonium oxalate extraction (data not shown) methods accounted for  $18 \pm 11\%$  and  $23 \pm 9\%$  of total Fe, in EAV floc and RAS, respectively and  $10 \pm 3\%$  and  $29 \pm 9\%$  of total Fe in SAV floc and RAS, respectively. These results suggest that the large proportion of Fe is complexed with organic matter or occluded with  $\text{CaCO}_3$  and stored in a stable pool (Boyd and Ellwood, 2010; Colombo et al., 2014; Lalonde et al., 2012). Similarly, extraction of Al using HCl and oxalate extraction methods accounted for  $34 \pm 9\%$  and  $18 \pm 8\%$  of total Al in EAV floc and RAS and  $36 \pm 15\%$  and  $21 \pm 13\%$  of total Al in SAV floc and RAS, respectively. The role of Fe and Al and underlying mechanisms needs further investigation to determine if these metals are involved in binding P in high Ca systems such as SAV.

All minerals identified or tentatively identified in the samples analyzed have been previously reported to occur in the greater Everglades region (Das et al., 2012; Farve et al., 2004; Harris et al., 2007; Olila et al., 1995). The lack of P mineral detection does not preclude their presence in trace amounts, as suggested by SEM-EDS data. Even P concentrations of  $>1000 \text{ mg kg}^{-1}$  (the case for 4 of the 6 samples analyzed) were marginal with respect to detecting phosphate minerals via XRD. Also, their detection may have been masked by elevated scan backgrounds from organic matter and other non-crystalline components.

The SEM-EDS analyses confirming Ca-P associations were only performed on two RAS samples from the inflow and midpoint of the EAV FW in this study. However, SEM-EDS analyses revealed a common occurrence of Ca-P particles in the silt fraction of Lake Okeechobee mud sediment (Harris et al., 2007). The nature and provenance of this Ca-P phase (or phases) are pertinent to P dynamics in the Greater Everglades region. They could be allochthonous such that their presence in the STA is more a consequence of hydrodynamics than of biogeochemical processes internal to the STA. Alternatively, they could be the result of Ca-P precipitation as fostered by conditions within the STA.

#### 4.2.2. Non-reactive phosphorus (NRP)

The chemical composition of NRP is unknown because of methodology and instrumentation limitations. For example, key inorganic P compounds that may be included in this pool are P-minerals and stable precipitates in SAV samples which are not extracted with the chemicals used in the fractionation. Similarly, the efficiency of organic P extraction via NaOH-EDTA, as shown via  $^{31}\text{P}$  NMR is between 40 and 60% of total P. Thus, organic P forms identified in our study are limited to organic P extraction efficiency and do not represent total organic P (Cade-Menun and Liu, 2014; Cheesman et al., 2014). It is likely that most of the NRP in EAV soils is dominated by organic form, as this system is driven by accretion of organic matter and associated nutrients. Organic P stored in NRP can be mined by microbes and plants through various processes including enhanced enzyme activity, photosynthetic C inputs into roots, fresh organic matter inputs through litter, and nutrient loading. These factors are known to enhance the decomposition of stable organic matter through the priming effect (Fontaine et al., 2011, 2007).

#### 4.3. Management implications

The loads experienced by the FWs over the past 14 years resulted in substantial P enrichment in floc and RAS layers as compared to underlying native pre-STA soils at locations in the first-half of the flow-path (up to 2 km from inflow) as compared to the second half of the flow-path. In floc and RAS, HRP accounts approximately 24% of total P storage in EAV as compared to 29% in SAV, while RP accounts for 57% in both EAV and SAV systems. Approximately one-fourth of the P stored in upstream areas of EAV and SAV can serve as a significant source of P to the overlying water column.

Significant correlations were noted between floc labile Pi and overlying water column P forms with correlation coefficients in the range of 0.73 to 0.80 ( $P < 0.01$ ; Reddy et al., 2019). Inorganic P released during mineralization of organic P also maintains high porewater P levels and potentially results in upward P flux into the overlying water column (Reddy et al., 2005). High concentrations of labile Pi in P enriched areas in the upper portion of EAV and SAV FWs suggest that floc and RAS maintain high porewater P concentrations, which can result in upward flux into the water column. The HRP pool can be a major source of internal P load to the water column, until this pool is transformed into a stable pool (Adhikari et al., 2015). In the SAV system, the night time absence of underwater photosynthesis can create high carbon dioxide concentrations at the soil-water interface and potentially solubilize occluded P and release it into porewater, followed by upward flux into the overlying water column (Scinto and Reddy, 2003).

For STAs to continue to function effectively and meet the desired outflow TP concentrations, management strategies should be aimed to promote P limiting conditions within the system to avoid release of P from floc and soils to water column and potential downstream transport.

#### 5. Conclusions

Phosphorus pools determined by conventional fractionation methods provided information on discrete pools of inorganic and organic P as influenced by vegetation and nutrient loading. Steady loading of P into the STAs has increased the relative proportion of all forms of soil P, with the largest proportion stored in slowly available and refractory forms of organic P. No phosphate minerals were detected by XRD, but SEM-EDS elemental dot maps and point spectra showed small discrete Ca-P particles. There was no obvious diffuse association of P with Ca such as via structural impurity or surface interactions with carbonates, but P concentrations were likely too low to document such forms. Dominance of  $\text{CaCO}_3$  in SAV system promoted the accretion of P and associated elements. Organic pools of P identified by conventional methods were to some extent confirmed by the  $^{31}\text{P}$  NMR spectroscopy. In EAV, significant correlations were observed between organic P pools and phosphomonoesters and diesters, while in SAV MBC showed significant correlation with diesters, suggesting some validation between two methods.

Phosphorus loading increased the proportion of P stored as inorganic P in SAV system and as organic P in EAV system. Upstream areas of FWs are once adapted to high P use efficiency under P limiting conditions are now transformed to a lower P use efficiency as a result of P enriched conditions and accumulation HRP and RP pools, suggesting that surplus P can be a source of internal P load. For STAs to function effectively to meet the desired outflow TP concentrations, it is important to develop management strategies to keep them under P assimilating conditions to avoid P leakage to the water column and downstream transport.

Management of HRP pool in floc and RAS is critical to reduce mobility of P into overlying water column and potential transport to downstream areas of STAs. Selection of vegetation and flow-paths in operating STAs should focus on stabilizing HRP and RP pools. Using synergistic roles of EAV and SAV, flow-path vegetation patterns in STAs can

potentially be modified to better stabilize HRP and RP pools and reduce the risk of P leakage in upstream areas into the water column. This could be done by establishing a ridge (with EAV) and slough (SAV) type of environment in STA flow-paths.

### CRediT authorship contribution statement

**K.R. Reddy:** Conceptualization, Methodology, Writing - original draft, Writing - review & editing, Resources, Funding acquisition. **Lilit Vardanyan:** Investigation, Writing - review & editing. **Jing Hu:** Investigation, Writing - original draft, Writing - review & editing. **Odi Villapando:** Writing - review & editing. **Rupesh Bhomia:** Investigation, Writing - review & editing. **Taylor Smith:** Investigation. **W.G. Harris:** Writing - review & editing, Investigation. **Sue Newman:** Writing - review & editing.

### Declaration of competing interest

The authors declare that they have no known competing financial interests or personal relationships that could have appeared to influence the work reported in this paper.

### Acknowledgments

This research work was conducted during 2015–2019 in compliance with the agreement between the South Florida Water Management District (SFWMD) and the University of Florida and (UF Contract #460003031-WO01). It is part of the UF Collaborative Research Initiative Science Plan with the SFWMD for the Everglades Stormwater Treatment Areas (CRESTA) and supports the Restoration Strategies Science Plan for the Everglades STAs. A portion of this work was performed at the National High Magnetic Field Laboratory, which is supported by the National Science Foundation Cooperative Agreement No. DMR-1644779 and the State of Florida and in part by an NIH award, S10RR031637, for magnetic resonance instrumentation. Authors appreciate the review of this manuscript by Ms. Jill King from the SFWMD. We acknowledge the assistance of Mr. Andres Trucco (UF Nanoscale Research Facility) and Ms. Elizabeth Stanley (UF-SWS-Soil Mineralogy Laboratory). We thank Mr. Jim Rocca, Advanced Magnetic Resonance Imaging and Spectroscopy (AMRIS) Facility, UF-McKnight Brain Institute for his technical assistance in <sup>31</sup>P NMR spectroscopy.

### References

Adhikari, P.L., White, J.R., Maiti, K., Nguyen, N., 2015. Phosphorus speciation and sedimentary phosphorus release from the Gulf of Mexico sediments: implication for hypoxia. *Estuar. Coast. Shelf Sci.* 164, 77–85. <https://doi.org/10.1016/j.eccs.2015.07.016>.

Andersen, M.R., Sand-Jensen, K., Iestyn Woolway, R., Jones, I.D., 2017. Profound daily vertical stratification and mixing in a small, shallow, wind-exposed lake with submerged macrophytes. *Aquat. Sci.* 79, 395–406. <https://doi.org/10.1007/s00027-016-0505-0>.

Bhomia, R.K., Reddy, K.R., 2018. Influence of vegetation on long-term phosphorus sequestration in subtropical treatment wetlands. *J. Environ. Qual.* 47, 361–370. <https://doi.org/10.2134/jeq2017.07.0272>.

Bhomia, R.K., Inglett, P.W., Reddy, K.R., 2015. Soil and phosphorus accretion rates in subtropical wetlands: Everglades stormwater treatment areas as a case example. *Sci. Total Environ.* 533, 297–306. <https://doi.org/10.1016/j.scitotenv.2015.06.115>.

Boyd, P.W., Ellwood, M.J., 2010. The biogeochemical cycle of iron in the ocean. *Nat. Geosci.* 3, 675–682. <https://doi.org/10.1038/ngeo964>.

Bünemann, E.K., 2015. Assessment of gross and net mineralization rates of soil organic phosphorus - a review. *Soil Biol. Biochem.* <https://doi.org/10.1016/j.soilbio.2015.06.026>.

Cade-Menun, B., Liu, C.W., 2014. Solution phosphorus-31 nuclear magnetic resonance spectroscopy of soils from 2005 to 2013: a review of sample preparation and experimental parameters. *Soil Sci. Soc. Am. J.* 78, 19–37. <https://doi.org/10.2136/sssaj2013.05.0187dgs>.

Celi, L., Barberie, E., 2005. Abiotic stabilization of organic phosphorus in the environment. In: Turner, B.L., Frossard, E., Baldwin, D.S. (Eds.), *Organic Phosphorus in the Environment*. CAB International, Wallingford, UK, pp. 113–132.

Celi, L., Barberis, E., 2007. Abiotic reactions of inositol phosphates in soil. In: Turner, B.L., Richardson, A.E., Mullaney, E.J. (Eds.), *Inositol Phosphates: Linking Agriculture and the Environment*. CAB International, Wallingford, UK, pp. 207–220.

Cheesman, A.W., Rocca, J., Turner, B.L., 2013. Chapter 33. Phosphorus characterization in wetland soils by solution phosphorus-31 nuclear magnetic resonance spectroscopy. In: DeLaune, R.D., Reddy, K.R., Richardson, C.J., Megonigal, J.P. (Eds.), *Methods in*

*Biogeochemistry of Wetlands*. SSSA Book Series, no. 10. Soil Science Society of America, 5585 Guilford Road, Madison, WI, pp. 639–665.

Cheesman, A.W., Turner, B.L., Reddy, K.R., 2014. Forms of organic phosphorus in wetland soils. *Biogeochemistry* 11, 6697–6710. <https://doi.org/10.5194/bg-11-6697-2014>.

Chimney, M.J., 2019. Chapter 5B: Performance and operation of the Everglades stormwater treatment areas. South Florida Environmental Report. South Florida Water Management District, West Palm Beach, pp. 1–36 5B.

Chimney, M.J., Pietro, K.C., 2006. Decomposition of macrophyte litter in a subtropical constructed wetland in south Florida (USA). *Ecol. Eng.* 27, 301–321. <https://doi.org/10.1016/j.ecoleng.2006.05.016>.

Colombo, C., Palumbo, G., He, J.Z., Pinton, R., Cesco, S., 2014. Review on iron availability in soil: interaction of Fe minerals, plants, and microbes. *J. Soils Sediments* 14, 538–548. <https://doi.org/10.1007/s11368-013-0814-z>.

Condron, L.M., Newman, S., 2011. Revisiting the fundamentals of phosphorus fractionation of sediments and soils. *J. Soils Sediments* 11, 830–840. <https://doi.org/10.1007/s11368-011-0363-2>.

Condron, L.M., Turner, B.L., Cade-Menun, B.J., 2005. Chemistry and dynamics of soil organic phosphorus. In: Sims, J.T., Sharpley, A.N. (Eds.), *Phosphorus: Agriculture and the Environment*. American Society of Agronomy, Madison, WI, pp. 87–121.

Das, J., Daroub, S.H., Bhadha, J.H., Lang, T.A., Diaz, O., Harris, W., 2012. Physicochemical assessment and phosphorus storage of canal sediments within the Everglades Agricultural Area, Florida. *J. Soils Sediments* 12, 952–965. <https://doi.org/10.1007/s11368-012-0508-y>.

DeBusk, W.F., Reddy, K.R., 2005. Litter decomposition and nutrient dynamics in a phosphorus enriched everglades marsh. *Biogeochemistry* 75, 217–240. <https://doi.org/10.1007/s10533-004-7113-0>.

DeBusk, W.F., Reddy, K.R., Koch, M.S., Wang, Y., 1994. Spatial distribution of soil nutrients in a Northern Everglades marsh: water conservation area 2A. *Soil Sci. Soc. Am. J.* 58, 543–552. <https://doi.org/10.2136/sssaj1994.03615995005800020042x>.

Farve, M., Harris, W., Dierberg, F., Portier, K., 2004. Association between phosphorus and suspended solids in an Everglades treatment wetland dominated by submersed aquatic vegetation. *Wetl. Ecol. Manag.* 12, 365–375. <https://doi.org/10.1007/s11273-004-4447-2>.

Fontaine, S., Barot, S., Barré, P., Bdioui, N., Mary, B., Rumpel, C., 2007. Stability of organic carbon in deep soil layers controlled by fresh carbon supply. *Nature* 450, 277–280. <https://doi.org/10.1038/nature06275>.

Fontaine, S., Henault, C., Aamor, A., Bdioui, N., Bloor, J.M.G., Maire, V., Mary, B., Revallot, S., Maron, P.A., 2011. Fungi mediate long term sequestration of carbon and nitrogen in soil through their priming effect. *Soil Biol. Biochem.* 43, 86–96. <https://doi.org/10.1016/j.soilbio.2010.09.017>.

Hamad, M.E., Rimmer, D.L., Syers, J.K., 1992. Effect of iron oxide on phosphate sorption by calcite and calcareous soils. *J. Soil Sci.* 43, 273–281. <https://doi.org/10.1111/j.1365-2389.1992.tb00135.x>.

Harris, W.G., White, G.N., 2008. X-ray diffraction techniques for soil mineral identification. In: Ulery, A., Drees, R. (Eds.), *Methods of Soil Analysis: Part 5 - Mineralogical Methods*. Soil Sci. Soc. Am, Madison, WI, pp. 81–115.

Harris, W.G., Fisher, M.M., Cao, X., Osborne, T., Ellis, L., 2007. Magnesium-rich minerals in sediment and suspended particulates of South Florida water bodies: implications for turbidity. *J. Environ. Qual.* 36, 1670–1677. <https://doi.org/10.2134/jeq2006.0559>.

Harris, W.G., Smith, T., Bhomia, R., Villapando, O., Reddy, K.R., 2019. Section 7: mineralogical composition of STA soils and particulate matter of surface water. UF-WBL 2019. Evaluation of Soil Biogeochemical Properties Influencing Phosphorus Flux in the Everglades Stormwater Treatment Areas (STAs). Final Report. Work Order 460003031-WO01. 7. South Florida Water Management District, West Palm Beach, FL, pp. 1–27.

Hedley, M.J., Stewart, J.W.B., 1982. Method to measure microbial phosphate in soils. *Soil Biol. Biochem.* 14, 377–385. [https://doi.org/10.1016/0038-0717\(82\)90009-8](https://doi.org/10.1016/0038-0717(82)90009-8).

Hietljes, A.H.M., Lijklema, L., 1980. Fractionation of inorganic phosphates in calcareous sediments. *J. Environ. Qual.* 9, 405–407. <https://doi.org/10.2134/jeq1980.00472425000900030015x>.

Huang, L., Zhang, Y., Shi, Y., Liu, Y., Wang, L., Yan, N., 2015. Comparison of phosphorus fractions and phosphatase activities in coastal wetland soils along vegetation zones of Yancheng National Nature Reserve, China. *Estuar. Coast. Shelf Sci.* 157, 93–98. <https://doi.org/10.1016/j.eccs.2014.09.027>.

Ivanoff, D.B., Reddy, K.R., Robinson, J.S., 1998. Chemical fractionation of organic P in selected Histosols. *Soil Sci.* 163, 36–45. <https://doi.org/10.1097/00010694-199801000-00006>.

Kadlec, R.H., Bevis, F.B., 2009. Wastewater treatment at the Houghton Lake wetland: vegetation response. *Ecol. Engineering.* 35, 1312–1332.

Kadlec, R.H., Wallace, S.D., 2009. *Treatment Wetlands*. Second edition. CRC Press, Boca Raton, FL.

Koch, M., Kruse, J., Eichler-Löbermann, B., Zimmer, D., Willbold, S., Leinweber, P., Siebers, N., 2018. Phosphorus stocks and speciation in soil profiles of a long-term fertilizer experiment: evidence from sequential fractionation, P K-edge XANES, and <sup>31</sup>P NMR spectroscopy. *Geoderma* 316, 115–126. <https://doi.org/10.1016/j.geoderma.2017.12.003>.

Lalonde, K., Mucci, A., Ouellet, A., Gélinas, Y., 2012. Preservation of organic matter in sediments promoted by iron. *Nature* 483, 198–200. <https://doi.org/10.1038/nature10855>.

Maharjan, M., Maranguit, D., Kuzyakov, Y., 2018. Phosphorus fractions in subtropical soils depending on land use. *Eur. J. Soil Biol.* 87, 17–24. <https://doi.org/10.1016/j.ejsobi.2018.04.002>.

Miao, S.L., Sklar, F.H., 1998. Biomass nutrient allocation of sawgrass and cattails along a nutrient gradient in the Florida Everglades. *Wetland Ecology and Management* 5, 245–263.

Moore, P.A., Reddy, K.R., 1994. Role of Eh and pH on phosphorus geochemistry in sediments of Lake Okechobee, Florida. *J. Environ. Qual.* 23, 955–964. <https://doi.org/10.2134/jeq1994.00472425002300050016x>.

- Morris, J.T., Barber, D.C., Callaway, J.C., Chambers, R., Hagen, S.C., Hopkinson, C.S., Johnson, B.J., Megonigal, P., Neubauer, S.C., Troxler, T., Wigand, C., 2016. Contributions of organic and inorganic matter to sediment volume and accretion in tidal wetlands at steady state. *Earth's Futur* 4, 110–121. <https://doi.org/10.1002/2015EF000334>.
- Newman, S., Osborne, T.Z., Hagerthey, S.E., Saunders, C., Rutchey, K., Schall, T., Reddy, K.R., 2017. Drivers of landscape evolution: multiple regimes and their influence on carbon sequestration in a sub-tropical peatland. *Ecol. Monogr.* 87, 578–599. <https://doi.org/10.1002/ecm.1269>.
- Noe, G.B., Childers, D.L., Jones, R.D., 2001. Phosphorus biogeochemistry and the impact of phosphorus enrichment: why is the Everglades so unique? *Ecosystems* 4, 603–624. <https://doi.org/10.1007/s10021-001-0032-1>.
- Noe, G.B., Childers, D.L., Edwards, A.L., Gaiser, E., Jayachandran, K., Lee, D., Meeder, J., Richards, J., Scinto, L.J., Trexler, J.C., Jones, R.D., 2002. Short-term changes in phosphorus storage in an oligotrophic Everglades wetland ecosystem receiving experimental nutrient enrichment. *Biogeochemistry* 59, 239–267. <https://doi.org/10.1023/A:1016090009874>.
- Oberson, A., Joner, E.J., 2005. Microbial turnover of phosphorus in soil. In: Turner, B.L., Frossard, E., Baldwin, D.S. (Eds.), *Organic Phosphorus in the Environment*. CABI, Wallingford, UK, pp. 133–164.
- Olila, O.G., Reddy, K.R., Harris, W.G., 1995. Forms and distribution of inorganic phosphorus in sediments of two shallow eutrophic lakes in Florida. *Hydrobiologia* 302, 147–161. <https://doi.org/10.1007/BF00027039>.
- Pedersen, O., Colmer, T.D., Sand-Jensen, K., 2013. Underwater photosynthesis of submerged plants - recent advances and methods. *Front. Plant Sci.* 4, 140. <https://doi.org/10.3389/fpls.2013.00140>.
- Pelechaty, M., Pukacz, A., Apolinarska, K., Pelechata, A., Siepak, M., 2013. The significance of Chara vegetation in the precipitation of lacustrine calcium carbonate. *Sedimentology* 60, 1017–1035. <https://doi.org/10.1111/sed.12020>.
- Qualls, R.G., Heyvaert, A.C., 2017. Accretion of nutrients and sediment by a constructed stormwater treatment wetland in the Lake Tahoe Basin. *JAWRA J. Am. Water Resour. Assoc.* 53, 1495–1512. <https://doi.org/10.1111/1752-1688.12595>.
- Reddy, K.R., DeLaune, R.D., 2008. *Biogeochemistry of Wetlands: Science and Applications*. CRC Press, Boca Raton, FL, USA.
- Reddy, K.R., Wang, Y., DeBusk, W.F., Fisher, M.M., Newman, S., 1998. Forms of soil phosphorus in selected hydrologic units of the Florida Everglades. *Soil Sci. Soc. Am. J.* 62, 1134. <https://doi.org/10.2136/sssaj1998.03615995006200040039x>.
- Reddy, K.R., White, J.R., Wright, A., Chua, T., 1999. Influence of phosphorus loading on microbial processes in soil and water column of wetlands. In: Reddy, K.R., O'Conner, G.A., Schelske, C.L. (Eds.), *Phosphorus Biogeochemistry in Subtropical Ecosystems: Florida as a Case Example*. CRC/Lewis Pub, pp. 249–273.
- Reddy, K.R., Wetzel, R.G., Kadlec, R.H., 2005. Biogeochemistry of phosphorus in wetlands. In: Sims, J.T., Sharpley, A.N. (Eds.), *Phosphorus: Agriculture and the Environment*. American Society of Agronomy, Madison, WI, pp. 263–316.
- Reddy, K.R., Chua, T., Richardson, C.J., 2013. Chapter 35: organic phosphorus mineralization in wetland soils. In: DeLaune, R.D., Reddy, K.R., Richardson, C.J., Megonigal, P.J. (Eds.), *Methods in Biogeochemistry of Wetlands*, Book Series No. 10. Soil Science Society of America, Madison, WI, pp. 683–700.
- Reddy, K.R., Vardanyan, L., Hu, J., Villapando, O., Bhomia, R., Smith, T., Osborne, T., 2019. Section 5: soil phosphorus forms. UF-WBL 2019. Evaluation of Soil Biogeochemical Properties Influencing Phosphorus Flux in the Everglades Stormwater Treatment Areas (STAs). Final Report. Work Order 4600003031-WO01, South Florida Water Management District, West Palm Beach, FL. 6, pp. 1–160.
- Reid, R.J., Mosley, L.M., 2016. Comparative contributions of solution geochemistry, microbial metabolism and aquatic photosynthesis to the development of high pH in ephemeral wetlands in South East Australia. *Sci. Total Environ.* 542, 334–343. <https://doi.org/10.1016/j.scitotenv.2015.10.040>.
- Richardson, A.E., Simpson, R.J., 2011. Soil microorganisms mediating phosphorus availability. *Plant Physiol.* 156, 989–996. <https://doi.org/10.1104/pp.111.175448>.
- Ruttenberg, K.C., 1992. Development of a sequential extraction method for different forms of phosphorus in marine sediments. *Limnol. Oceanogr.* 37, 1460–1482. <https://doi.org/10.4319/lo.1992.37.7.1460>.
- Ruttenberg, K.C., 2003. The global phosphorus cycle. *Treatise on Geochemistry*. Elsevier Inc, pp. 585–643. <https://doi.org/10.1016/B0-08-043751-6/08153-6>.
- Ryan, J., Curtin, D., Cheema, M.A., 1985. Significance of iron oxides and calcium carbonate particle size in phosphate sorption by calcareous soils. *Soil Sci. Soc. Am. J.* 49, 74–76. <https://doi.org/10.2136/sssaj1985.03615995004900010014x>.
- Scinto, L.J., Reddy, K.R., 2003. Biotic and abiotic uptake of phosphorus by periphyton in a subtropical freshwater wetland. *Aquat. Bot.* 77, 203–222. [https://doi.org/10.1016/S0304-3770\(03\)00106-2](https://doi.org/10.1016/S0304-3770(03)00106-2).
- Siong, K., Asaeda, T., Fujino, T., Redden, A., 2006. Difference characteristics of phosphorus in Chara and two submerged angiosperm species: implications for phosphorus nutrient cycling in an aquatic ecosystem. *Wetl. Ecol. Manag.* 14, 505–510. <https://doi.org/10.1007/s11273-006-9003-9>.
- Solis, P., Torrent, J., 1989. Phosphate sorption by calcareous vertisols and inceptisols of Spain. *Soil Sci. Soc. Am. J.* 53, 456–459. <https://doi.org/10.2136/sssaj1989.03615995005300020024x>.
- Song, N., Yan, Z.-S., Cai, H.-Y., Jiang, H.-L., 2013. Effect of temperature on submerged macrophyte litter decomposition within sediments from a large shallow and subtropical freshwater lake. *Hydrobiologia* 714, 131–144. <https://doi.org/10.1007/s10750-013-1529-2>.
- Torres, I.C., Turner, B.L., Ramesh Reddy, K., 2014. The chemical nature of phosphorus in subtropical Lake sediments. *Aquat. Geochemistry* 20, 437–457. <https://doi.org/10.1007/s10498-014-9228-9>.
- Torres, I.C., Turner, B.L., Reddy, K.R., 2017. Phosphatase activities in sediments of subtropical lakes with different trophic states. *Hydrobiologia* 788, 305–318. <https://doi.org/10.1007/s10750-016-3009-y>.
- Turner, B.L., Newman, S., 2005. Phosphorus cycling in wetland soils: the importance of phosphate diesters. *J. Environ. Qual.* 34, 1921–1929. <https://doi.org/10.2134/jeq2005.0060>.
- Turner, B.L., Papházy, M.J., Haygarth, P.M., McKelvie, I.D., 2002. Inositol phosphates in the environment. *Philos. Trans. R. Soc. B Biol. Sci.* 357, 449–469. <https://doi.org/10.1098/rstb.2001.0837>.
- Turner, B.L., Newman, S., Newman, J.M., 2006. Organic phosphorus sequestration in subtropical treatment wetlands. *Environ. Sci. Technol.* 40, 727–733. <https://doi.org/10.1021/es0516256>.
- USEPA, 1983. *Methods for Chemical Analysis of Water and Wastes*. Environ. Monit. Support Lab, Cincinnati, OH, USA.
- Watson, S.J., Cade-Menun, B.J., Needoba, J.A., Peterson, T.D., 2018. Phosphorus forms in sediments of a river-dominated estuary. *Front. Mar. Sci.* 5, 302. <https://doi.org/10.3389/fmars.2018.00302>.
- Weng, S., Putz, G., Kells, J.A., 2006. Phosphorus uptake by cattail plants in a laboratory-scale experiment related to constructed treatment wetlands. *J. Environmental Engineering and Science* 5, 295–308. <https://doi.org/10.1139/s05-030.2006>.
- Yang, X., Post, W.M., 2011. Phosphorus transformations as a function of pedogenesis: a synthesis of soil phosphorus data using Hedley fractionation method. *Biogeosciences* 8, 2907–2916. <https://doi.org/10.5194/bg-8-2907-2011>.
- Zhao, Hongying, Piccone, Tracey, 2020. Large scale constructed wetlands for phosphorus removal, an effective nonpoint source pollution treatment technology. *Ecological Engineering* 145 (15), 105711. <https://doi.org/10.1016/j.ecoleng.2019.105711>.
- Zhu, J., Li, M., Whelan, M., 2018. Phosphorus activators contribute to legacy phosphorus availability in agricultural soils: a review. *Sci. Total Environ.* 612, 522–537. <https://doi.org/10.1016/j.scitotenv.2017.08.095>.